THE JOURNAL OF BIOLOGICAL CHEMISTRY VOL. 289, NO. 24, pp. 16711–16726, June 13, 2014

A Novel Intracellular Peptide Derived from G_1/S Cyclin D2 Induces Cell Death*[S]

Received for publication, November 21, 2013, and in revised form, April 23, 2014 Published, JBC Papers in Press, April 24, 2014, DOI 10.1074/jbc.M113.537118

Christiane B. de Araujo[‡1], Lilian C. Russo[¶], Leandro M. Castro[‡], Fábio L. Forti[¶], Elisabete R. do Monte[‡], Vanessa Rioli[‖], Fabio C. Gozzo[**], Alison Colquhoun[§], and Emer S. Ferro[‡2]

From the Departments of [‡]Pharmacology and [§]Cell Biology and Development, Support Center for Research in Proteolysis and Cell Signaling (NAPPS), Biomedical Science Institute, University of São Paulo, São Paulo, 05508-000, SP, Brazil, the [¶]Department of Biochemistry, Support Center for Research in Proteolysis and Cell Signaling (NAPPS), Institute of Chemistry, University of São Paulo, 05508-000, São Paulo, SP, Brazil, the [‖]Special Laboratory of Applied Toxinology (LETA), Center of Toxins, Immune Response, and Cell Signaling (CETICS), Butantan Institute, 05503-000, São Paulo, SP, Brazil, and the [**]Institute of Chemistry, State University of Campinas, 13083-862, Campinas, SP, Brazil

Background: Intracellular peptides probably regulate several biological processes.
Results: pep5 derived from G_1/S cyclin D2 specifically increases during the S phase of the cell cycle and, reintroduced into the cell, induces apoptosis and necrosis.
Conclusion: pep5 has potential therapeutic applications and could have biological functions.
Significance: pep5 discovery advances our understanding of limited proteolysis.

Intracellular peptides are constantly produced by the ubiquitin-proteasome system, and many are probably functional. Here, the peptide WELVVLGKL (pep5) from G_1/S-specific cyclin D2 showed a 2-fold increase during the S phase of HeLa cell cycle. pep5 (25–100 μM) induced cell death in several tumor cells only when it was fused to a cell-penetrating peptide (pep5-cpp), suggesting its intracellular function. *In vivo*, pep5-cpp reduced the volume of the rat C6 glioblastoma by almost 50%. The tryptophan at the N terminus of pep5 is essential for its cell death activity, and N terminus acetylation reduced the potency of pep5-cpp. WELVVL is the minimal active sequence of pep5, whereas Leu-Ala substitutions totally abolished pep5 cell death activity. Findings from the initial characterization of the cell death/signaling mechanism of pep5 include caspase 3/7 and 9 activation, inhibition of Akt2 phosphorylation, activation of p38α and -γ, and inhibition of proteasome activity. Further pharmacological analyses suggest that pep5 can trigger cell death by distinctive pathways, which can be blocked by IM-54 or a combination of necrostatin-1 and q-VD-OPh. These data further support the biological and pharmacological potential of intracellular peptides.

Cell signaling induces modification of the protein interactome network. The ubiquitin-proteasome system is responsible for maintaining protein homeostasis in cells, and among its essential functions is its involvement with cancer biology and the immune system. The proteasome is responsible for the initial cleavage of antigenic proteins and the generation of the major histocompatibility complex class I (MHC-I)-bound antigens, which can later be trimmed within the endoplasmic reticulum by endoplasmic reticulum aminopeptidases to produce the correct N terminus to interact with the MHC-I (1, 2). In cancer biology, the ubiquitin-proteasome system is important for cell cycle progression because it targets cyclins for degradation (3). Proteasome inhibition is used clinically for the treatment of certain types of cancer and is the treatment of choice for multiple myeloma (4). Protein degradation by the proteasome generates intermediate peptides shown to contain from 2 to 21 amino acids (5, 6), which in theory suggests that cells are continually producing large quantities of peptides containing 2–21 amino acids. However, according to current knowledge, only one peptide from each cellular protein would escape post-proteasome proteolytic degradation to be presented at the cell surface bound to the MHC-I, suggesting that ~10,000 peptides cover the mammalian cell surface to allow self-recognition by the immune system (7, 8). Thus, almost the entire protein is believed to be recycled to amino acids within cells. Indeed, in yeast, mammalian cells, and flies, the injurious consequences of proteasome inhibition are rescued by amino acid supplementation, revealing the importance of the proteasome system in amino acid recycling for *de novo* protein synthesis (9). Further reports have suggested that peptides produced by the proteasome have a half-life of seconds (10–12). In specific circumstances, the ubiquitin-proteasome system can perform limited proteolysis, such as in the generation of the active dimeric NFκB transcriptional complexes (13).

Therefore, it is clear that the proteasome can perform both extensive and limited proteolysis, depending on the protein substrate. In our laboratory, we have shown that the proteasome could play a more extensive role in limited proteolysis than previously anticipated, generating intracellular peptides (14–16). These findings were based on a well established con-

* This work was supported by Brazilian National Research Council (CNPq) Grant 559698/2009-7 (Rede GENOPROT) and by the Pro-Reitoria de Pesquisa, University of São Paulo, through the Support Center for Research in Proteolysis and Cell Signaling (NAPPS; Grant 2012.1.17607.1.2).
[S] This article contains supplemental data.
[1] Recipient of research fellowship from CAPES.
[2] Recipient of research fellowship from CNPq. To whom correspondence should be addressed: Dept. of Pharmacology, University of São Paulo. Av. Prof. Lineu Prestes 1524, S315, Cid. Universitária, SP, 05508-000, Brazil. Tel.: 55-11-3091-7493; Fax: 55-11-3091-7322; E-mail: eferro@usp.br.

cept that rationally designed peptides, structurally similar to the ones produced by the proteasome, can regulate protein spatial localization within cells and control cell signal transduction (17, 18). As such, naturally occurring intracellular peptides generated by the proteasome would constitute an as yet poorly understood mechanism by which cells increase their protein network complexity and function (16). Hemopressin, the first intracellular peptide identified using this rationale (19), was shown to have cannabinoid inverse agonist action regulating food intake (20, 21), whereas the natural brain hemopressins are secreted and suggested to play an important role as novel endocannabinoids (14, 22).

Later it was shown that intracellular peptides can function in modulating signal transduction from inside the cells because peptides structurally related to proteasome products were identified by mass spectrometry, chemically synthesized, and reintroduced into cells, where they modulated both angiotensin II and β-adrenergic signal transduction (23). These peptides were used for affinity chromatography and were suggested to bind to a specific set of proteins, many involved in protein and vesicular traffic (23). In addition to the proteasome, thimet oligopeptidase (EC 3.4.24.15; EP24.15), which is an intracellular peptidase that only degrades small peptides (~5–17 amino acids), was also shown to participate in intracellular peptide metabolism (24). By manipulating intracellular EP24.15 activity either by overexpressing the enzyme or inhibiting its activity by means of siRNA, it was possible to modulate G-protein-coupled receptor signal transduction in HEK293 and CHO-S cells (23, 25). These data suggest a previously unknown connection between intracellular peptide metabolism and signal transduction. Other signal transduction pathways could also be related to intracellular peptides because two similar peptides identified in the Wistar rat adipose tissue where shown to bind specific proteins and facilitate insulin-induced glucose uptake in 3T3-L1 adipocyte cells (26). Although the intracellular peptides have not yet been shown to directly modulate protein-protein interactions *in vivo*, the *in vitro* use of surface plasmon resonance demonstrates that at concentrations of 1–50 μM, several intracellular peptides can modulate the interactions of calmodulin and 14-3-3ϵ with proteins from the mouse brain cytoplasm or with recombinant EP24.15. One of these peptides (VFDVELL; VFD-7), shown to be a proteasome product (24), increases the free cytosolic Ca^{2+} concentration in a dose-dependent manner but only if introduced into HEK293 cells (27).

In the present report, we aim to obtain further information on the cell biology and therapeutic potential of intracellular peptides by investigating their possible participation in the cell cycle. To that end, we identified in extracts of HeLa cells a novel peptide fragment (WELVVLGKL; pep5) that specifically increases during the S phase of the cell cycle and is derived from the G_1/S-specific cyclin D2 protein. The peptide pep5 induces cell death in HeLa and several other tumor cells and *in vivo* reduces by 50% the volume of the rat C6 glioblastoma. Collectively, the above results suggest that peptides generated by the proteasome and additional intracellular peptidases need further attention as novel natural modulators of cell function. These data suggest the therapeutic potential of intracellular peptides.

EXPERIMENTAL PROCEDURES

Reagents—Acetonitrile was purchased from Fisher. Mass spectrometry grade hydrochloric acid and trifluoroacetic acid were from Pierce. Hydroxylamine, glycine, sodium hydroxide, sodium phosphate, dimethyl sulfoxide (DMSO), necrostatin-1, q-VD-OPh (qVD),[3] and IM-54 were obtained from Sigma. The 4-trimethylammoniumbutyryl (TMAB)-*N*-hydroxysuccinimide-stable isotopic labeling reagents, containing either 0, 3, or 9 atoms of deuterium (D0, D3, and D9, respectively) or 9 atoms of deuterium and three ^{13}C atoms (D12) were synthesized as described by Che *et al.* (28), Morano *et al.* (29) and Zhang *et al.* (30). Fluorescamine and SB203580 were purchased from Invitrogen. All peptides were provided by Proteimax Biotechnology LTDA (São Paulo, Brazil).

Cell Lines—HeLa, MDA-MB-231, MCF-7, and C6 cells were cultured in Dulbecco's modified Eagle's medium (DMEM; Invitrogen), whereas SKRB, SK-MEL 28, MEL 85, SBCl-2, TPC-1, Nthy-ori 3-1, and KTC-2 cells were cultured in RPMI 1640 (Invitrogen) at 37 °C and 5% of CO_2, containing 10% fetal bovine serum (complete medium), penicillin, and streptomycin (Invitrogen).

Cell Cycle Synchronization by Double-thymidine Block—HeLa cells were synchronized using the double-thymidine block procedure (31, 32). Thymidine (Sigma-Aldrich) was diluted in serum-free DMEM and stored at 4 °C before use. For cell cycle synchronization, HeLa cells were treated with 2 mM thymidine for 18 h and washed in phosphate-buffered saline (PBS), cell medium was replaced with complete medium, and cells were cultured for an additional 9 h at 37 °C and 5% of CO_2. The above procedure was repeated once more to arrest cells in S phase. At different times (4, 10, and 16 h, at which ~84% of cells were in S, G_1, and G_2/M phases, respectively) cells were harvested, analyzed by flow cytometry, and submitted to additional assays. Control cells were asynchronous.

Flow Cytometry—Cell cycle was analyzed by flow cytometry using a Guava Easy City Mini Flow Cytometry (Millipore) instrument. Cells were fixed in 70% ethanol for 1 h and incubated with propidium iodide (1 mg/ml) and RNase (10 mg/ml) for 30 min on ice, and a total of 10,000 events were analyzed in each sample.

Cell Morphology Analyses—HeLa cells (4×10^5 cells/plate) were grown in 35-mm cell culture dishes (Corning Inc.) in complete medium and treated with scrambled control peptide (SCB), pep5, cell-penetrating peptide (cpp), SCB-cpp, or pep5-cpp (50 or 100 μM) for 24 h. After that, cell morphology was visualized and photographed under an inverted phase-contrast microscope (Zeiss Axiovert 25 inverted phase contrast microscope) at ×400 magnification.

Apoptosis Assay—Cells were treated with pep5-cpp, cpp alone, and ΔN or ΔC-pep5-cpp for 10 or 30 min. After incubation, cells were harvested and washed in cold phosphate-buffered saline (PBS) and resuspended in 100 μl of 1× annexin-binding buffer (Molecular Probes). Alexa Fluor® 488 annexin V (5 μl) was added with 1 μl of 100 μg/ml PI working solution to each 100 μl of

[3] The abbreviations used are: qVD, quinolyl-Val-Asp-OPh; TMAB, 4-trimethylammoniumbutyryl; cpp, cell-penetrating peptide; SCB, scrambled control peptide.

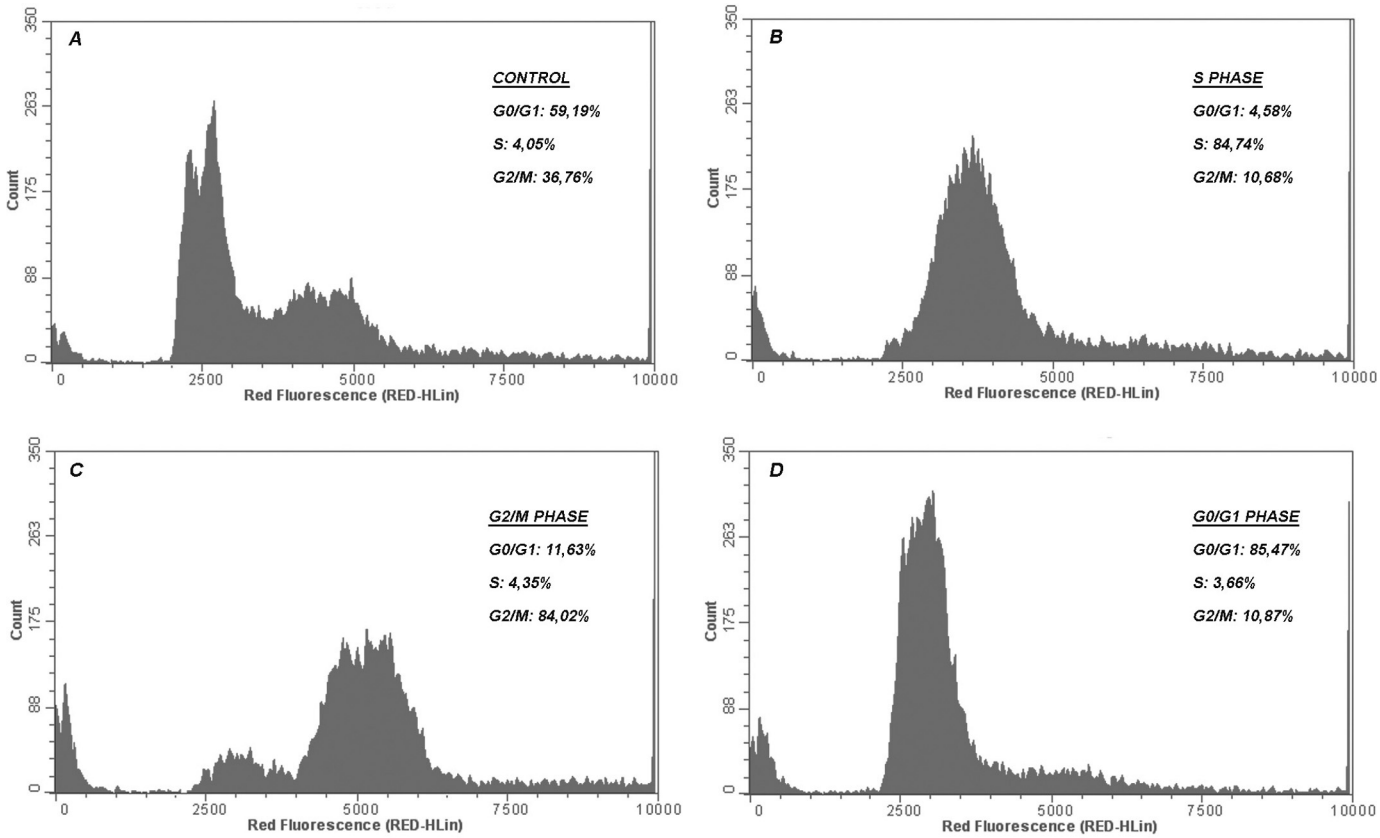

FIGURE 1. **Synchronization of HeLa cells using 2 mM thymidine.** The percentage of the cells in each phase was determined by flow cytometry analysis. DNA content frequency histograms represent cells in S, G_2/M, and G_1, respectively, 4, 10, and 16 h after double thymidine block or asynchronous growing cells in the control culture. Fluorescence intensity was measured after adding propidium iodide to the cells. The histograms and the graph (mean and S.E. (*error bars*)) shown here are representative of three independent experiments. *A*, control (asynchronous cells); *B–D*, cells synchronized in S, G_2/M, and G_1 phases.

TABLE 1

Summary of protein precursors and sequence of the peptides identified in HeLa cells along the progression of the cell cycle

Protein name, precursor protein of the respective peptide sequence; pep#, peptide identity, according to the order in which it was sequenced; Sequence, the respective peptide sequence identified by MS/MS analyses (all of the MS and MS/MS spectra are presented in the supplemental material); *z*, the peptide charge state; #T, the number of tags in the identified peptide; Obs M, observed mass; Theor M, theoretical mass of the peptide; ppm, mass accuracy; Ratio, relative level of each peptide in the specific cell cycle phase indicated (G_1, S, or G_2)/control asynchronous cells. Except for peptides 16 and 18, all data presented are mean ± S.E.; $n = 4$. MS and MS/MS data are given in the supplemental material.

Protein name	pep#	Sequence	*z*	#T	Obs M	Theor M	ppm	Ratio		
								G_1/CT	S/CT	G_2/CT
Peptidyl-prolyl cis-trans isomerase A	1	ADKVPKTAENFR	4	3	1,374.7	1,374.7	−13.4	1.19 ± 0.24	2.11 ± 2.13	1.75 ± 1.17
40 S ribosomal protein S21	2	KADGIVSKNF	3	3	1,077.5	1,077.6	−52.4	0.71 ± 0.21	0.69 ± 0.13	0.83 ± 0.08
40 S ribosomal protein S21	3	AKADGIVSKNF	3	3	1,148.6	1148.6	−45,0	1.52 ± 0.41	1.95 ± 0.14	1.88 ± 0.32
40 S ribosomal protein S21	4	GSGSKGKGGEIQPVSV	3	3	1,485.7	1485.8	−62.7	1.39 ± 0.51	1.57 ± 1.16	1.29 ± 0.96
G_1/S-specific cyclin D2	5	WELVVLGKL	2	2	1,055.5	1055.6	−164.2	1.27 ± 0.67	2.16 ± 0.40	1.22 ± 0.47
TOX high mobility group box family member 3	6	QITSPIPAIGS	3	1	1,082.6	1082.6	10.4	0.70 ± 0.30	0.58 ± 0.06	1.24 ± 0.62
40 S ribosomal protein S21	7	ADGIVSKNF	2	2	949.4	949.5	−73.1	0.98 ± 0.27	0.94 ± 0.32	0.85 ± 0.17
Polypyrimidine tract-binding protein 1	8	RIIVENL	3	1	855.5	855.5	−64.4	1.15 ± 0.12	1.19 ± 0.04	1.61 ± 0.44
Activated RNA polymerase II transcriptional coactivator p15	9	KEQISDIDDAVRKL	4	3	1,628.8	1,628.9	−45.0	1.60 ± 0.39	1.94 ± 0.12	1.84 ± 0.39
PPIA_HUMAN, peptidyl-prolyl *cis-trans*-isomerase A	10	AVDGEPLGRVSF	2	1	1,245.6	1,245.6	−52,4	0.71 ± 0.28	0.69 ± 0.33	0.83 ± 0.18
Potassium channel subfamily T member 1	11	SILLNPGPRHILA	2	1	1,399.4	1,399.8	−286.5	0.84 ± 0.06	0.71 ± 0.19	0.76 ± 0.16
Dipeptidyl peptidase 1	12	DPFNPFELTNH	2	1	1,329.8	1,329.6	162.9	0.96 ± 0.08	0.33 ± 0.46	0.66 ± 0.93
Hemopexin	13	LTKGGYTL	2	2	851.4	851.5	−115,6	0.61 ± 0.09	0.57 ± 0.63	0.41 ± 0.35
Cytochrome *c* oxidase subunit 5A, mitochondrial	14	GISTPEELGLDKV	2	2	1,356.6	1,356.7	−52.2	0.62 ± 0.14	0.49 ± 0.20	0.51 ± 0.12
Cofilin-1	15	GGSAVISLEGKPL	2	2	1,226.6	1,226.7	−59.7	1.14 ± 0.01	1.07 ± 0.23	1.03 ± 0.17
Lysosomal protective protein	16	APDQDEIQR	2	1	1,070.5	1,070.5	−39.2	0.46	0.73	0.71
Protocadherin α-3	17	GEGLPKTDL	2	2	928.4	928.5	−86.7	0.82 ± 0.16	0.83 ± 0.04	0.97 ± 0.08

cell suspension. The samples were incubated at room temperature for 15 min, and after the incubation period, 400 μl of 1× annexin-binding buffer were added, mixed gently, and kept on ice. As soon as possible, the samples were analyzed by flow cytometry, measuring the fluorescence emission at 530 and >575 nm.

Surgery—C6 rat glioma (*Rattus norvegicus*) (33) cells were grown in DMEM containing 10% fetal bovine serum and antibiotics (penicillin/streptomycin). Cells in the exponential phase of growth were used, and a suspension was prepared in sterile saline at a concentration of 5×10^5 cells/4–5 μl. Adult male

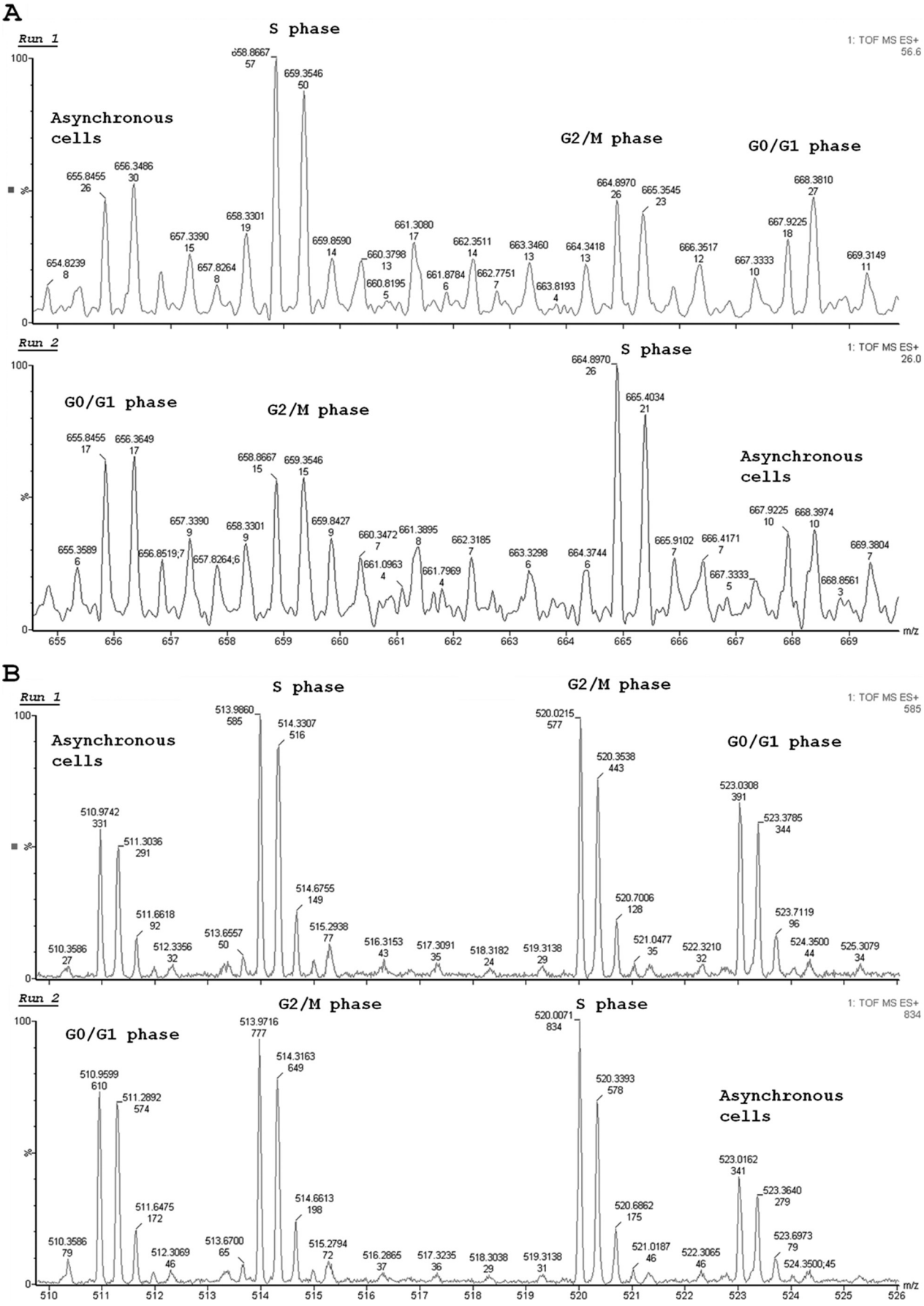
A
Run 1
S phase
1: TOF MS ES+
56.6
Asynchronous cells
G2/M phase
G0/G1 phase
Run 2
S phase
1: TOF MS ES+
26.0
G0/G1 phase
G2/M phase
Asynchronous cells
m/z
B
Run 1
S phase
G2/M phase
1: TOF MS ES+
585
Asynchronous cells
G0/G1 phase
Run 2
G2/M phase
S phase
1: TOF MS ES+
834
G0/G1 phase
Asynchronous cells
m/z

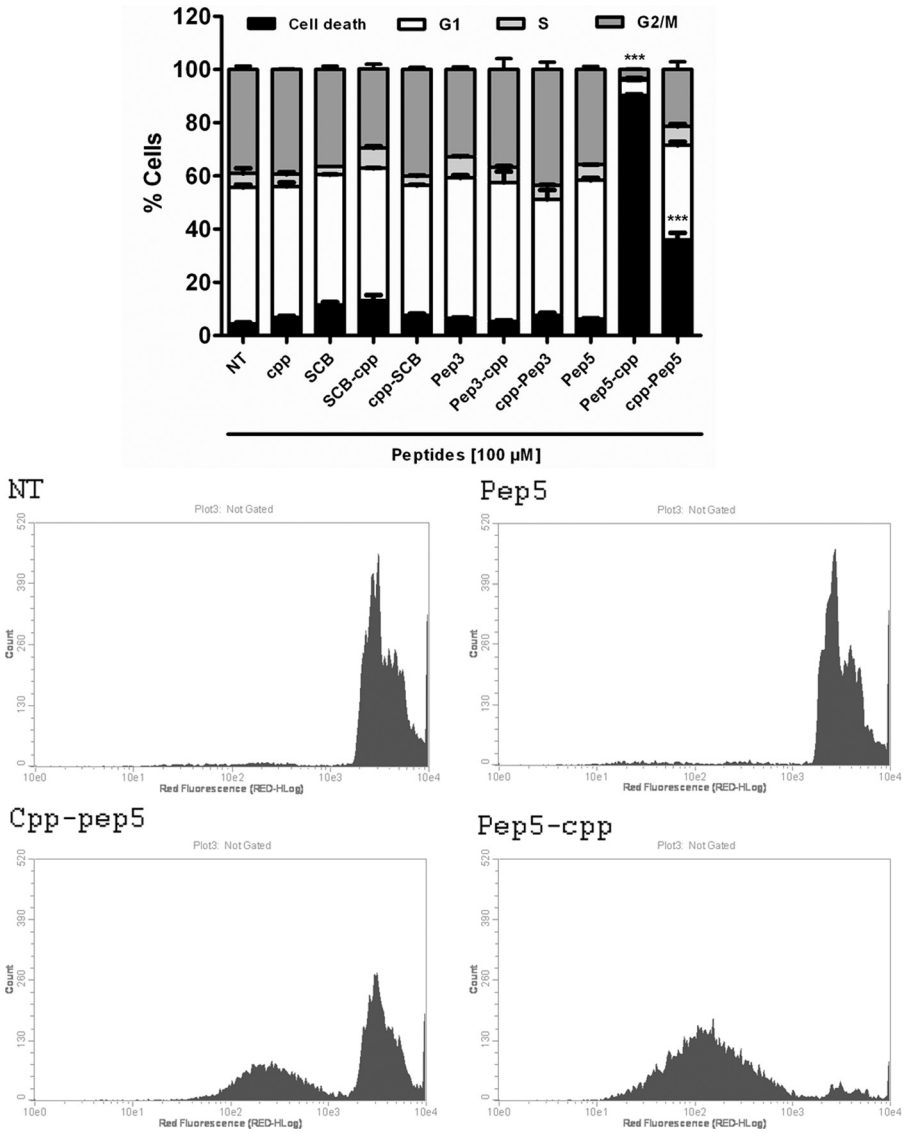

FIGURE 3. **Effect of intracellular peptides in HeLa cells.** HeLa cells were treated with peptide 3 or 5 free or fused to a cpp, cpp alone, or SCB for 24 h. After that, the cells were fixed in 70% ethanol and analyzed by propidium iodide staining and flow cytometry. Results were considered significant when p was $\leq$0.001 (***). The data shown here are representative of three independent experiments performed in triplicate. *NT*, not treated; *pep-cpp*, cpp fused to the C terminus of the peptides; *cpp-pep*, cpp fused to the N terminus of the peptides. The histograms show the difference among the groups treated with pep5 bound or not to the cpp in the N or C terminus. *Error bars*, S.E.

Wistar rats of 250–350 g (n = 5) were anesthetized with an intramuscular injection of ketamine/xylazine (10 mg/1.5 mg/100 g of body weight) to provide deep anesthesia and analgesia. The rats were placed on a stereotaxic surgical table, a midline incision was made, and a burr hole was drilled 0.48 mm anterior and 3 mm lateral to the bregma. The C6 cell suspension was slowly injected into the striatum using a Hamilton syringe at a depth of 5.4 mm to the bone surface, and the needle was left *in situ* for 3 min before its removal. After 14 days, Alzet osmotic pumps containing either pep5-cpp or ΔN-pep5-cpp (100 μM) diluted in artificial cerebrospinal fluid were surgically implanted and attached to Alzet brain infusion kits. Artificial cerebrospinal fluid was chosen as a vehicle solution in order to mimic more closely the composition of the interstitial fluid within the brain. The peptide concentrations were chosen based on our previous results using cell lines. The pump infusion rate was 0.5 μl/h with a duration of 2 weeks. After a further 14 days, the rats were killed by transcardiac perfusion with 4% formaldehyde in 0.1 M phosphate buffer, pH 7.4.

After perfusion, the brains were removed, fixed in 4% formaldehyde, and cryoprotected with 30% sucrose in PBS. The frozen tissue sections (30 μm) were obtained on a freezing microtome. The brain slices were stained with H&E, and tumor area was analyzed under a microscope. The largest areas of tumor were measured using image analysis software (Image ProPlus). The volume was calculated using the formula, V =

FIGURE 2. **MS spectra representing the semiquantitative analysis of peptides from synchronized HeLa cell extracts (S, G_2/M, and G_1) or controls.** HeLa cells were synchronized with 2 mM thymidine, and the peptides were labeled with isotopes TMAB (D0, D3, D9, and D12). *A* and *B*, representative MS spectra of two peptides (pep5 and pep3) that reproducibly changed during the HeLa cell cycle. The data shown here are representative of two independent experiments.

$\pi/6 \times L \times W \times H$. This procedure was approved by the Ethical Commission for Animal Experimentation of the Biomedical Sciences Institute (University of São Paulo), protocol number 116/08.

Peptide Extraction and Quantification—HeLa cells (1×10^6 cells/plate) were grown in 10-cm cell culture plates (Corning Inc.) in complete medium. Fifteen plates of cells were used per group, and each group was characterized by flow cytometry to be in specific phases of the cell cycle, meaning asynchronous, G_1, S, or G_2/M. Complete medium was removed, and cells were washed three times with PBS, scraped from the plates, and centrifuged at $830 \times g$ for 5 min. The pellet was resuspended in 10 ml of 80 °C water and incubated in an 80 °C water bath for 20 min. The cell lysates were stored at −80 °C overnight. To extract peptides, samples were acidified with 10 μl of ice-cold 0.1 M HCl to a final concentration of 10 mM HCl and sonicated three times with 20 pulses (4 Hz) on ice. The samples were centrifuged at 2,500 rpm in a microcentrifuge for 40 min at 4 °C, and the supernatant was collected for peptide extraction. The supernatant was ultracentrifuged at 34,000 rpm for 60 min at 4 °C, transferred to a centrifugal filter device for the separation of molecules of less than 5,000 Da (Millipore), and centrifuged again at 2,500 rpm for 1 h at 4 °C. The peptide quantification reaction was performed at pH 6.8 to ensure that only the amino groups of peptides and not free amino acids reacted with fluorescamine, as described previously (23, 34). Briefly, 2.5 μl of peptide samples were mixed with 25 μl of 0.2 M phosphate buffer (pH 6.8) and 12.5 μl of a 0.3 mg/ml acetone fluorescamine solution. After vortexing for 1 min, 110 μl of water was added, and fluorescence was measured with a SpectraMax M2e plate reader (Molecular Devices) at an excitation wavelength of 370 nm and an emission wavelength of 480 nm. A peptide mixture of known composition and concentration was used as the standard reference for determining the peptide concentration in the experimental samples.

Isotopic Labeling and Mass Spectrometry for Peptide Identification—The labeling procedure has been previously described in detail (35, 36). In brief, each group of cells within an experiment was labeled with one of the isotopic TMAB-*N*-hydroxysuccinimide labels. The S, G_2/M, or G_1 groups of characterized cells were labeled with D3-, D9-, or D12-TMAB, respectively (Run 1), whereas the control asynchronous cells were labeled with D0-TMAB. This labeling was altered (reverse labeling) between experiments (Run 2). These two experiments above were performed independently. A total of 50 μg of the peptide extract was combined with 250 μl of 0.4 M phosphate buffer, pH 9.5, and 15 mg of TMAB label per group. After the addition of TMAB, the mixture was incubated at room temperature for an additional 60 min. To quench any remaining labeling reagent, 30 μl of 2.5 M glycine was added to the reaction. The sample was dried in a vacuum centrifuge and analyzed by liquid chromatography/mass spectrometry (LC-MS/MS) on a Synapt G1 mass spectrometer with a nanoACQUITY UltraPerformance LC System (Waters Co.). The MS spectra were analyzed using the MassLynx software (Waters) to identify groups of peaks representing peptides labeled with the different isotope tags. Quantification was performed by determining the relative intensity of each isotopic peak (37). To identify the peptides, the MS/MS data were analyzed using the Mascot search engine (Matrix Science Ltd.).

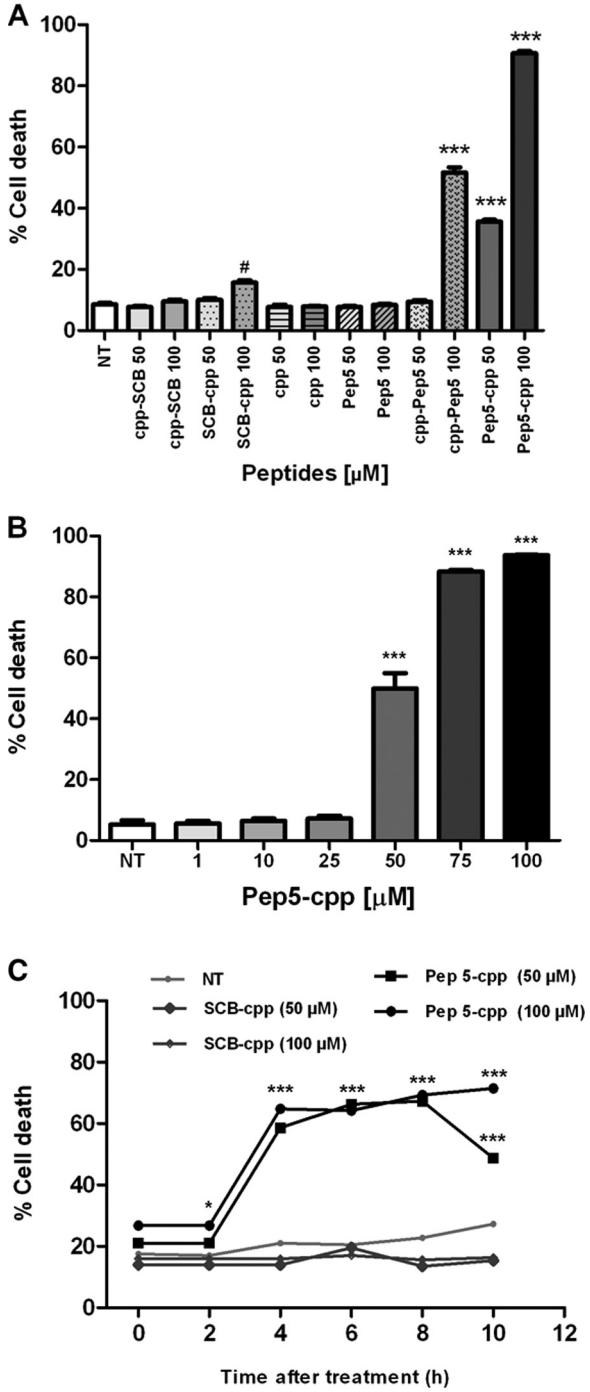

FIGURE 4. **Effect of pep5-cpp in HeLa cells.** *A*, HeLa cells were treated with peptide 5, cpp alone, or SCB for 24 h. *B*, cells were incubated with pep5-cpp at different concentrations (1, 10, 25, 50, 75 and 100 μM) for 24 h. *C*, cells were treated with pep5-cpp and SCB (control) for 10 h at 50 and 100 μM. After all tests, the cells were fixed in 70% ethanol and analyzed by propidium iodide staining and flow cytometry. Results were considered significant when p was ≤0.001 (***) or ≤0.05 (#). The data shown here are representative of three experiments performed in triplicate. *NT*, not treated; *pep-cpp*, cpp fused to the C terminus of the peptides; *cpp-pep*, cpp fused to the N terminus of the peptides. *Error bars*, S.E.

Peptide Synthesis—Peptides 3 and 5, whose concentrations were altered in different phases of the cell cycle, and a control

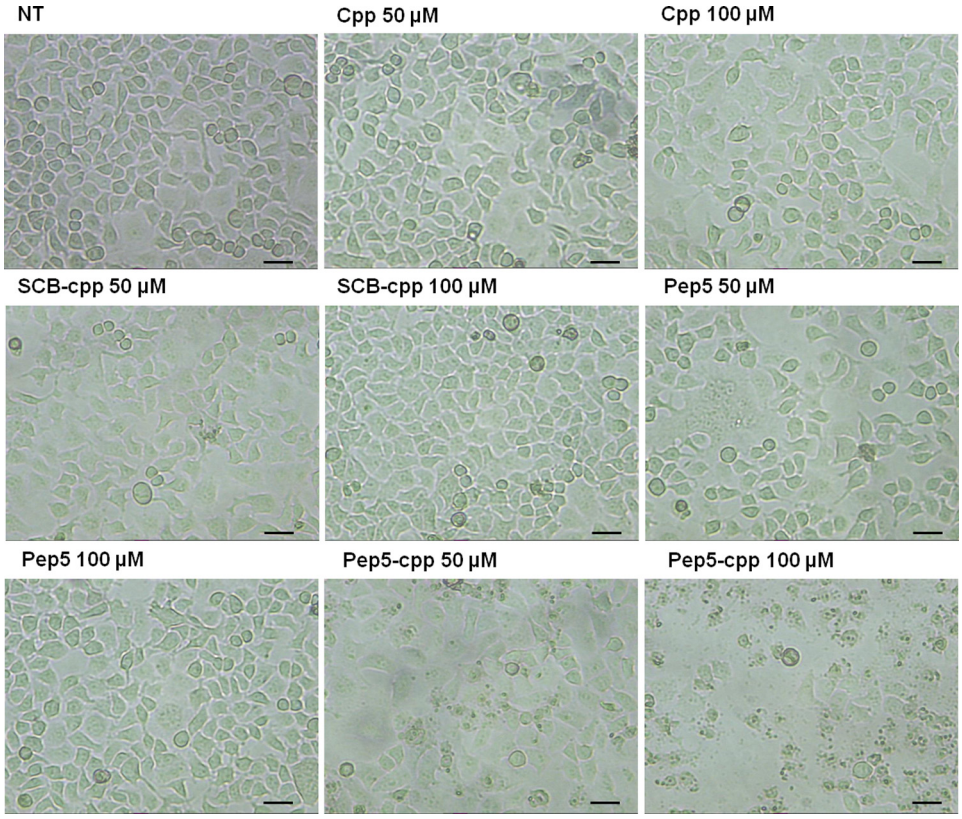

FIGURE 5. **Morphology of HeLa cells treated with pep5-cpp.** HeLa cells were treated or not with cpp, SCB, pep5, or pep5-cpp (50 and 100 μM) for 24 h. The cells were treated and photographed under an optical microscope after 24 h of treatment. The pictures show the difference in morphology of the cells treated or not with pep5-cpp (50 and 100 mM). *NT*, not treated. *Scale bar*, 50 μm.

scrambled peptide were synthesized with cpp (YGRKKRRQRRR) covalently bound to either their C or N terminus (38–40). In all assays, peptide purity was greater than 95%. All synthesized peptides were provided by Proteimax Biotechnology LTDA.

Caspase Assays—Caspase 3/7, 8, and 9 activities were evaluated in extracts of HeLa cells previously treated for 10 min with either the proapoptotic pep5-cpp or the control peptide (100 μM), using a commercial luminescent assay kit (Caspase-Glo® assay, Promega). The relative luminescence was measured in a SpectraMax luminometer (Molecular Devices).

Phospho-MAPK Array—A human phospho-MAPK array kit (Proteome Profiler) was used to simultaneously test pep5-cpp effects on the phosphorylation of diverse MAPK signaling pathways, according to instructions provided by the manufacturer. Briefly, all arrays were incubated with 200 μg of HeLa cell extracts treated previously for 10 min with either pep5-cpp or the control peptide (100 μM).

Pharmacological Treatments—HeLa cells (4×10^5 cells/plate) were pretreated with necrostatin-1 (nec-1), qVD, SB203580, or IM-54 (30 μM) for 1 h, and then pep5-cpp (75 μM) was added to the medium containing one or more inhibitors. After 4 h of treatment with pep5-cpp, cells were harvested and washed in PBS and analyzed by flow cytometry.

Proteasome Activity Assays—HeLa cells treated or not with pep5-cpp (50–200 μM) were washed twice with PBS and lysed on ice for 30 min. Cells extracts were centrifuged at 13,000 rpm for 10 min, and total protein concentration was determined by the Bradford assay (41) using bovine serum albumin as a standard. The proteasome substrate Glo™ Chymotrypsin-like (Suc-LLVY-Glo™, Promega) was used to determine the proteasome activity, as recommended by the manufacturer.

Statistics—Values are expressed as means ± S.E. Statistical analyses were conducted by Student's unpaired *t* test for independent samples or analysis of variance followed by Tukey's or Bonferroni's test to compare more than two groups, using GraphPad Prism version 5.0. *p* values of <0.05 were considered significant.

RESULTS

The initial hypothesis of our work was that the relative concentration of specific intracellular peptides, similarly to that of certain specific proteins, could vary throughout the cell cycle, and perhaps even contribute to its control. Therefore, we began by synchronizing HeLa cells using the double-thymidine block procedure (31, 32) to further isolate and characterize intracellular peptides from each individual phase of the cell cycle. As a result of the double-thymidine block, analyses by flow cytometry suggested that ~84% of HeLa cells were arrested in each phase of the cell cycle (G_1, S, or G_2/M) when compared with the asynchronous cell group (Fig. 1). The intracellular peptide content was then extracted from asynchronous, G_1, S, or G_2/M HeLa cells, labeled with specific TMAB isotopes, and analyzed by mass spectrometry. In these analyses, 19 peptides were sequenced and identified in order of appearance (Table 1; MS and MS/MS data are shown in the supplemental material).

pep3, a fragment from the 40 S ribosomal protein S21, and pep5, a fragment of G_1/S-specific cyclin D2 (Table 1), were observed to clearly fluctuate along the cell cycle (Fig. 2) and were further investigated with respect to their possible biological activity on regulating the progression of the cell cycle and/or cell survival. pep3, pep5, and SCB were chemically synthesized either free or covalently bound to a cpp at their C or N terminus. The cpp was necessary to allow cell penetration and consequent investigation of the possible intracellular function of these peptides. Moreover, the cpp used herein has been extensively described to transport its cargo into the cells (37, 38).

First, HeLa cells were treated with each of these peptides at a specific concentration (100 μM), and after 24 h, they were analyzed by flow cytometry (Fig. 3). The control peptides SCB and pep3, either free or bound to the cpp, or the cpp alone had no effect on cell cycle progression or cell death (Fig. 3). pep5 had no effect on cell cycle progression, whereas it killed ~90% of cells when cpp was linked to its C terminus and ~40% when cpp was linked to its N terminus (Fig. 3). A dose-response curve of pep5-cpp (1–100 μM) was performed in HeLa cells, showing cell death activity at concentrations above 50 μM (Fig. 4, *A* and *B*). A time course was also performed, indicating that pep5-cpp (50–100 μM) starts to induce significant cell death in HeLa cells after 2 h of incubation (Fig. 4*C*). HeLa cell morphology was observed following the treatments with SCB, pep5, cpp, SCB-cpp, or pep5-cpp (50 or 100 μM; 24 h). These results corroborate the suggestion that pep5-cpp at either 50 or 100 μM is inducing large cell death (Fig. 5).

Next we performed several modifications in the pep5 sequence to investigate the relationship between structure and activity. In order to identify the minimal active sequence, we started by deleting 1, 2, or 3 amino acids from either the N or C terminus. Removal of a single amino acid from the N terminus (ΔN-pep5-cpp) totally abolished the induction of cell death by pep5-cpp (Fig. 6). The potency of pep5-cpp was only slightly reduced by the removal of two or three amino acids from its C terminus, whereas it was totally abolished after the removal of four amino acids from the C terminus (Fig. 6*A*). Additional experiments were performed, substituting specific hydrophobic amino acids (Leu or Val) from the original sequence by Ala, which inactivated the cell death activity of pep5-cpp (Fig. 6*B*). pep5-cpp was also acetylated at the N terminus, and the results suggested that the cell death activity is retained, although with reduced potency compared with the original sequence (Fig. 6*C*). Table 2 summarizes the pep5-cpp sequences investigated herein. Taken together, these data suggest a strong structural specificity of pep5-cpp in inducing cell death.

To investigate whether the cell death induction caused by pep5-cpp was specific to HeLa cells, we investigated the effect of this peptide in additional tumor cell lines (Fig. 7). With distinctive efficacy, pep5-cpp (100 μM) induced cell death in all tumor cell lines investigated here (Fig. 7). The percentage of cell death caused by pep5-cpp was 81.5 ± 1.2% in SKRB (human breast cancer cell line), 94.7 ± 2.1% in SK-MEL-28 (human skin melanoma cell line), 84.6 ± 4.4% in SBCl-2 (human melanoma), 93.8 ± 1.7% in MEL-85 (human melanoma), 52.9 ± 9.7% in C6 (rat glial tumor), 82.1 ± 8.9% in TPC-1, and 84.9 ± 1.0% in KTC-2 (human thyroid tumor cell lines). The normal human thyroid cell line Nthy-ori 3-1 was also tested, and pep5-cpp killed 45.3 ± 3.0% of cells. Despite differences in efficacy, pep5-cpp was observed to induce cell death in all cell lines investigated (Fig. 7). Moreover, a dose-response curve was performed to investigate the effect of pep5-cpp in two distinctive human breast adenocarcinoma cell lines, MDA-MB-231 and MCF-7 (Fig. 8). These results suggest that MDA-MB-231 cells (Fig. 8*A*)

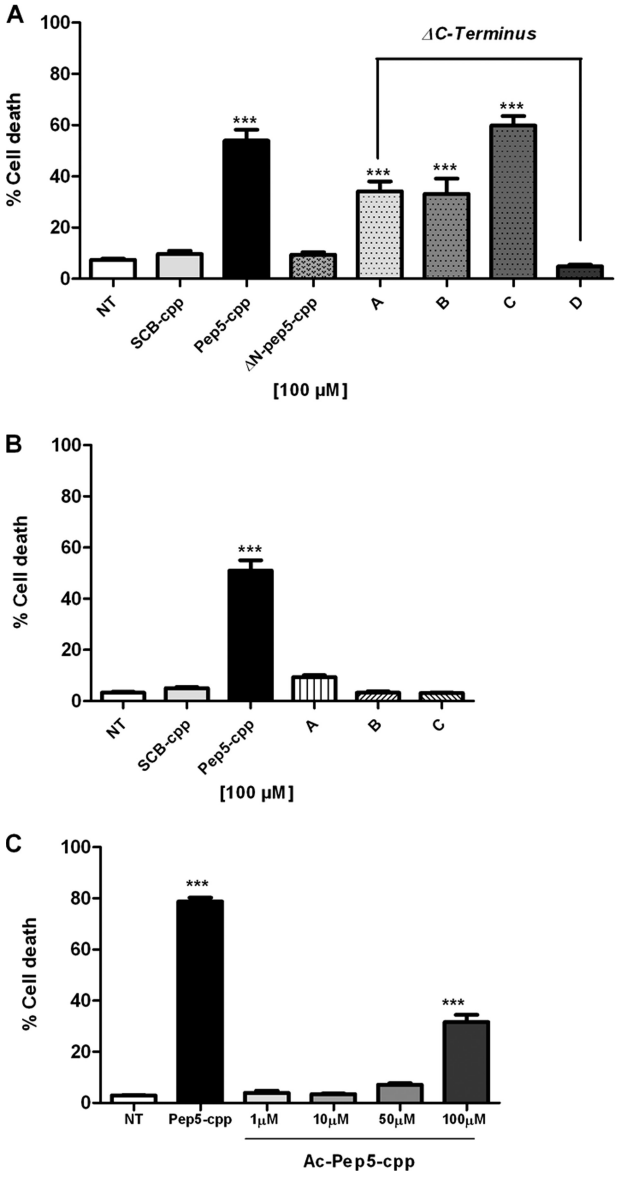

FIGURE 6. **Effect of modifications in the original sequence of pep5-cpp.** *A*, effect of deletions in pep5 sequence. Cells were treated with pep5-cpp, SCB (control), and ΔN- or ΔC-pep5-cpp (pep5 with deletions) for 24 h (100 μM) and then analyzed by flow cytometry. *NT*, not treated, SCB control; *ΔN-pep5-cpp*, deletion of one amino acid at the N terminus; *A*, *B*, *C*, and *D*, C terminus deletions of 1, 2, 3, and 4 amino acids, respectively. *B*, analysis of substitutions in the original sequence of pep5. Cells were treated with pep5-cpp, SCB, and a modified pep5-cpp for 24 h (100 μM) and then analyzed by flow cytometry. *A*, *B*, and *C*, pep5 with one or more substitutions, in the original sequence, for alanine. *C*, cells were treated with pep5-cpp (100 μM) and the acetylated pep5-cpp at different concentrations (1, 10, 50, and 100 μM) for 24 h and then analyzed by flow cytometry. *Ac-pep5-cpp*, acetylated pep5. The data shown here are representative of three experiments performed in triplicate, and the results were considered significant when p was <0.001 (***). *Error bars*, S.E.

TABLE 2

Amino acid sequences of pep5-cpp investigated herein

ΔN, one or more amino acids deleted from N terminus; ΔC, one or more amino acids deleted from C terminus; A, B, and C, amino acids substitutions for the minimal active sequence (ΔC_3-pep5-cpp*) of pep5-cpp. Ac-pep5-cpp, ΔC_3-pep5-cpp acetylated in the N terminus.

Amino acid sequences from pep5-cpp	Abbreviation
WELVVLGKL-YGRKKRRQRRR	pep5-cpp
ELVVLGKL-YGRKKRRQRRR	ΔN-pep5-cpp
LVVLGKL-YGRKKRRQRRR	ΔN_2-pep5-cpp
VVLGKL-YGRKKRRQRRR	ΔN_3-pep5-cpp
WELVVLGK-YGRKKRRQRRR	ΔC_1-pep5-cpp
WELVVLG-YGRKKRRQRRR	ΔC_2-pep5-cpp
WELVVL-YGRKKRRQRRR	ΔC_3-pep5-cpp*
WELVV-YGRKKRRQRRR	ΔC_4-pep5-cpp
WELV-YGRKKRRQRRR	ΔC_5-pep5-cpp
WEL-YGRKKRRQRRR	ΔC_6-pep5-cpp
WE-YGRKKRRQRRR	ΔC_7-pep5-cpp
WELVVA-YGRKKRRQRRR	A
WEAVVL-YGRKKRRQRRR	B
WEAVVA-YGRKKRRQRRR	C
Ac-WELVVL-YGRKKRRQRRR	Ac-pep5-cpp

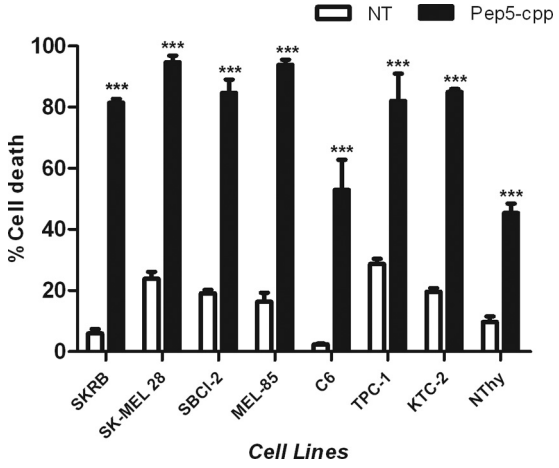

FIGURE 7. **Effect of pep5-cpp in several different cell lines.** *A*, cells were treated or not with pep5-cpp for 24 h (100 μM) and then analyzed by flow cytometry. *NT*, not treated. The data shown here are representative of three experiments performed in triplicate, and the results were considered significant when p was <0.001 (***). *Error bars*, S.E.

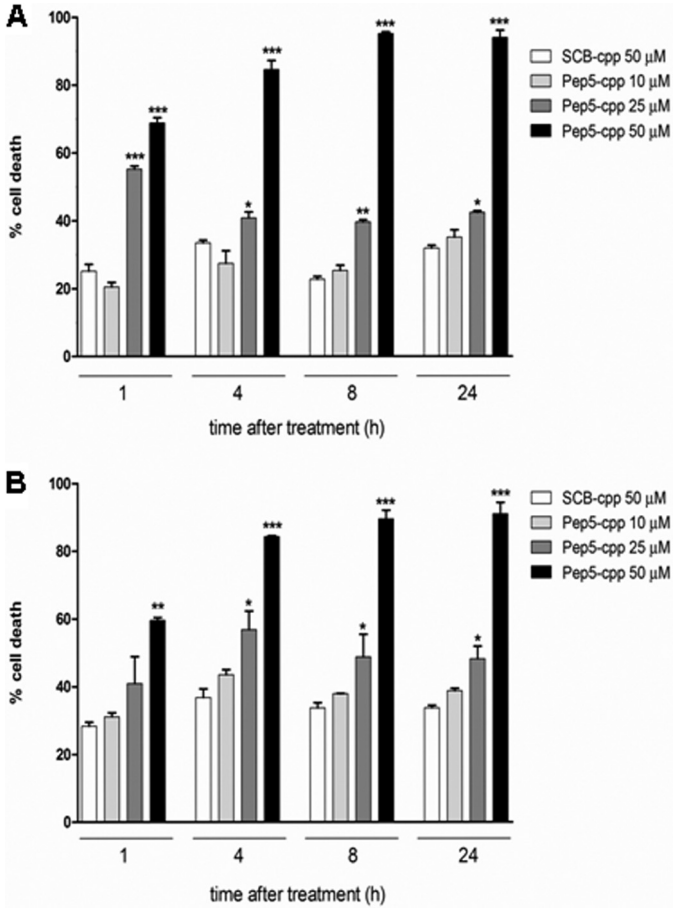

FIGURE 8. **Dose-response and time course of the cell death activity of pep5-cpp in MDA-MB-231 and MCF-7 tumor cell lines.** The MDA-MB-231 (*A*) or MCF-7 (*B*) cells were treated with pep5-cpp (1–50 μM) for different times (1–24 h). *NT*, not treated. The data shown here are representative of three experiments performed in triplicate, and the results were considered significant when p was <0.001 (***). *Error bars*, S.E.

are more sensitive than MCF-7 cells (Fig. 8*B*) to the cell death effects of pep5-cpp.

In vivo infusion of pep5-cpp (100 μM), but not ΔN-pep5-cpp (100 μM), caused a significant decrease in C6 tumor growth (Fig. 9). Whereas the average tumor volume in the ΔN-pep5-cpp-treated animals was 6.705 ± 1.20 mm^3, in the animals treated with pep5-cpp, it was only 3.404 ± 0.844 mm^3 (Fig. 9*A*), suggesting that pep5-cpp reduced the tumor volume by 49% ($p = 0.0275$, $n = 5$).

Next, we attempted to investigate the possible cell death-inducing mechanism of pep5-cpp. HeLa cells were treated with pep5-cpp or the cpp alone (50 μM) for 30 min and analyzed by flow cytometry in the presence of annexin V (Molecular Probes). Results suggest that pep5-cpp, but not cpp alone, significantly induces apoptosis and necrosis in HeLa cells (Fig. 10). After a 30-min treatment with pep5-cpp, apoptotic cells corresponded to ~30% of the total population, and necrotic cells corresponded to ~60%, whereas ~10% of the cells remained viable (Fig. 10*A*). Similar results were obtained using either pep5-cpp or its minimal active sequence (ΔC-pep5-cpp), which has three amino acids deleted from the C terminus (Fig. 10*B*). HeLa cells treated for 10 min with a lower dose of pep5-cpp (50 μM) showed no difference between apoptosis *versus* necrosis (Fig. 10*C*). Those cells treated with pep5-cpp (100 μM, 10 min) showed a significant increase of caspase 3/7 and 9 activities, whereas the activity of caspase 8 remained unaltered (Fig. 11). Treatment of HeLa cells with the control SCB peptide caused no cell death or caspase activation (Fig. 11).

Next, the mitogen-activated protein kinase (MAPK) pathway was evaluated in a standard array assay, which simultaneously investigates the phosphorylation of several kinases, including extracellular signal-regulated kinases (ERKs), c-Jun N-terminal or stress-activated protein kinases (JNK/SAPK), ERK/big MAP kinase 1 (BMK1), and the p38 kinases (42). HeLa cells were treated with pep5-cpp (100 μM, 10 min), the cell extracts were analyzed in duplicates according to the manufacturer's instructions, and the results were compared with untreated HeLa cells. Specific kinases or their substrates, such as ERK1/2, HSP27, p38 α/γ, and p70 S6 kinase had increased phosphorylation upon treatment with pep5-cpp, when compared with the untreated control group. However, substrates, such as Akt2 and GSK-3β, had decreased phosphorylation after treatment with pep5-cpp (Fig. 12*A*). Additional experiments were similarly conducted to

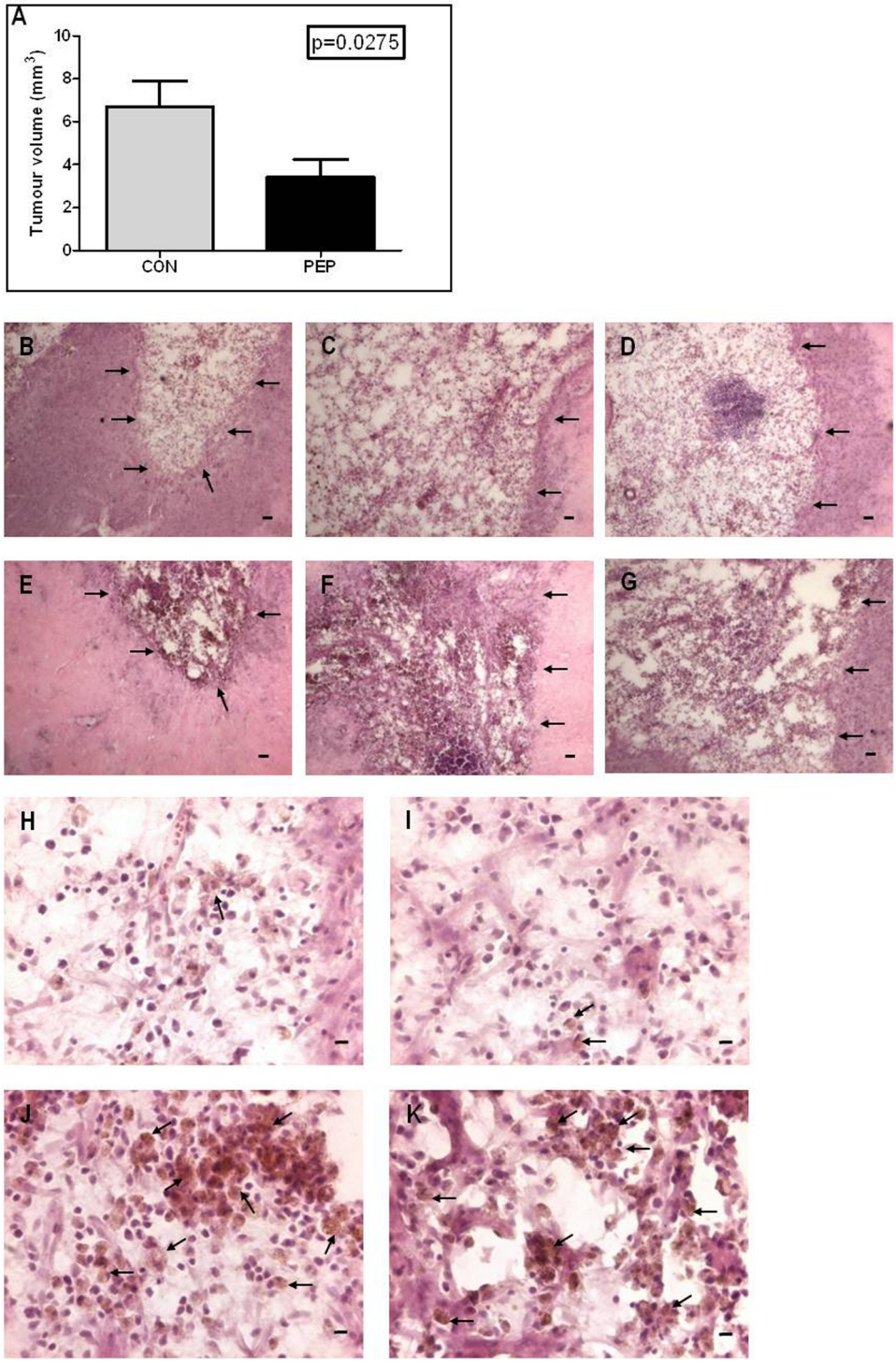

FIGURE 9. ***In vivo* effects of ΔN-pep5-cpp or pep5-cpp in the rat C6 glioma.** Male Wistar rats ($n = 5$) with 14-day pre-established tumors were treated with ΔN-pep5-cpp or pep5-cpp (100 μM) for an additional 14 days, and after infusion, the animals were killed with an overdose of ketamine-xylazine (Parke-Davis). After perfusion, the brains were removed, fixed in 4% formaldehyde, and cryoprotected with 30% sucrose in PBS. The frozen tissue sections (30 μm) were obtained on a freezing microtome. The brain slices were stained with H&E, and tumor area was analyzed under a microscope. The largest areas of tumor were measured using image analysis software (Image ProPlus). The volume was calculated using the formula, $V = \pi/6 \times L \times W \times H$. *A*, tumor volume. *B–D*, *H*, and *I*, ΔN-pep5-cpp. *E–G*, *J*, and *K*, pep5-cpp. *B–G*, *arrows* indicate tumor borders; *scale bar*, 400 μm. *J* and *K*, *arrows* indicate phagocytic macrophage-like cells. *Scale bar* (*H–K*), 20 μm. Analysis was done using the one-tailed *t* test, and the results were considered significantly different ($p = 0.0275$). *Error bars*, S.E.

compare the effect of cell death inducer pep5-cpp with the cell death-inactive ΔN-pep5-cpp; the latter peptide only lacks the original N-terminal amino acid residue from pep5-cpp. These results further suggest the structural specificity of pep5-cpp to inhibit Akt2 and to activate ERK2, HSP27, and p38γ phosphorylation (Fig. 12*B*).

The ability of pep5 to affect the chymotrypsin activity of the proteasome was evaluated both in whole cells and in cell extracts

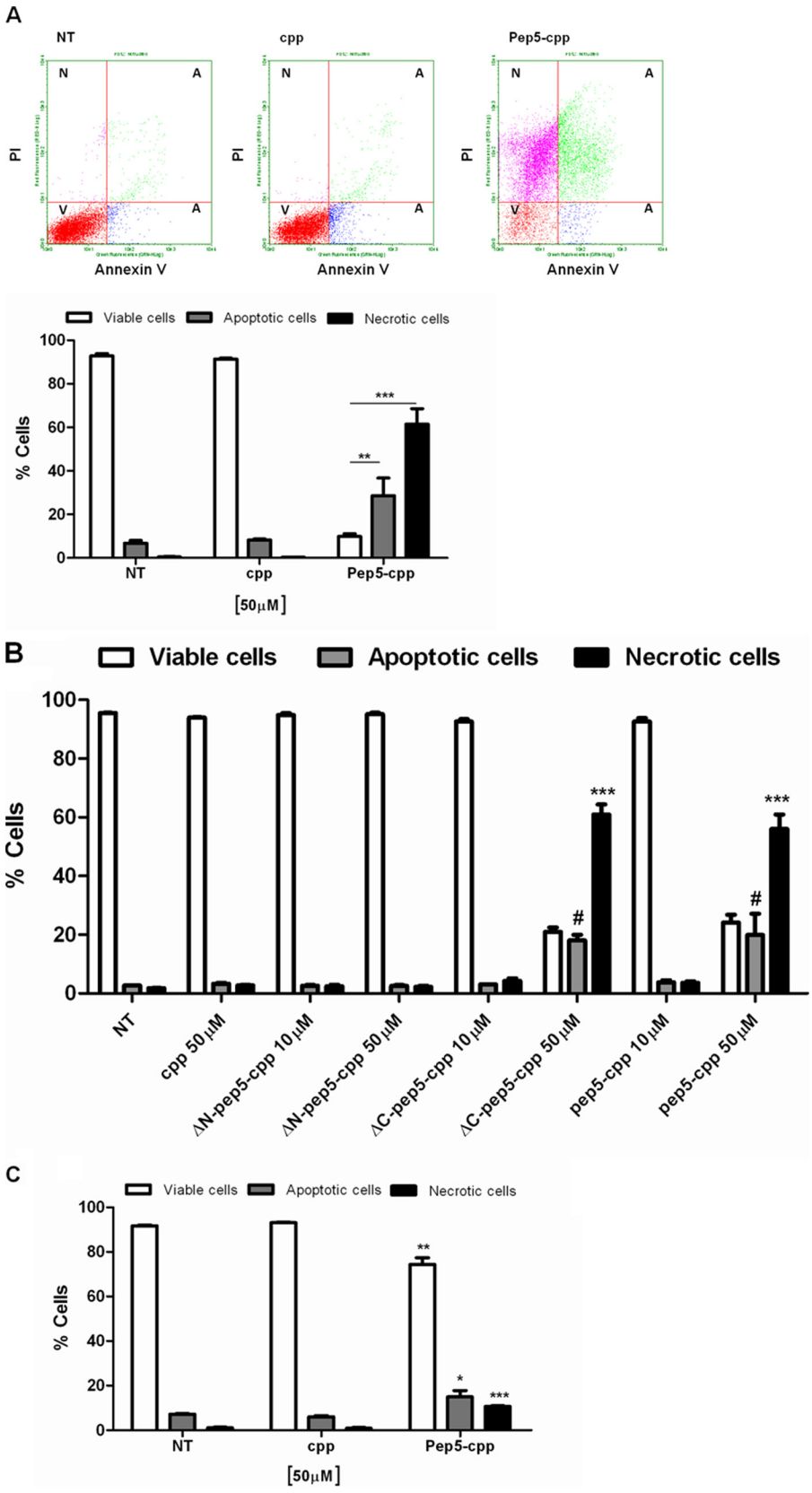

FIGURE 10. **Mechanism of cell death induced by pep5-cpp.** Cells were treated with cpp, pep5-cpp, or modified pep5-cpp (10–50 μM) for 30 min (*A* and *B*) or 10 min (*C*) and incubated with annexin V and propidium iodide (*PI*). After the incubation period (15 min), the samples were analyzed by flow cytometry. The population should separate into at least three groups: viable cells (*V*) with only a low level of fluorescence, apoptotic cells (*A*) with a substantially higher green fluorescence, and necrotic cells (*N*) with higher red fluorescence intensity. *NT*, not treated; Δ*N*- or Δ*C-pep5-cpp*, pep5 with deletions. The data shown here are representative of three experiments performed in triplicate, and the results were considered significant when p was <0.001 (***) or <0.05 (*). *Error bars*, S.E.

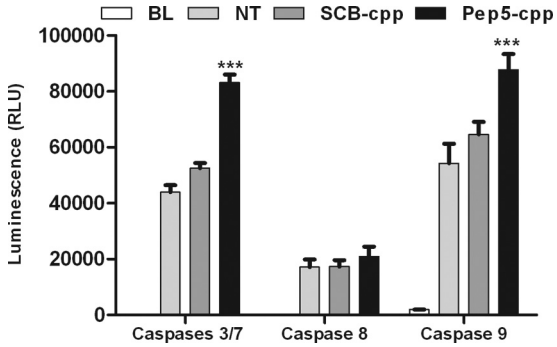

FIGURE 11. **Caspase assay after treatment with pep5-cpp.** Cells were treated with peptide 5 and SCB (scrambled) for 10 min (100 μM). After treatment, the substrates were added for the detection of different caspase activities. The relative luminescence was read using a luminometer (Spectramax, Molecular Devices). *BL*, blank; *NT*, not treated; *SCB*, control; *Pep5*, pep5-cpp. The data shown here are representative of three experiments performed in triplicate, and the results were considered significant when p was <0.001 (***). *RLU*, relative light units. *Error bars*, S.E.

using a standard commercial assay. In HeLa cells treated with pep5-cpp for 24 h, the proteasome activity was significantly reduced (Fig. 13*A*). pep5 also showed inhibitory activity of the chymotrypsin activity of the proteasome in cell extracts (Fig. 13*B*).

Furthermore, pharmacological treatments using distinctive inhibitors of cell death were conducted (Fig. 14). Necrostatin-1, an inhibitor of necroptosis (43); qVD, a potent caspase inhibitor that protects cells from capase-dependent apoptosis (44); SB203580, a selective inhibitor of p38 mitogen-activated protein kinase, which inhibits also the phosphorylation and activation of protein kinase B (PKB, also known as Akt1) (45, 46); and/or IM-54, a cell-permeable, potent, and selective inhibitor of oxidative stress-induced necrosis (47) were evaluated (30 μM, 1 h of pretreatment). Used alone, only the IM-54 significantly reduced the cell death induction caused by pep5-cpp. On the other hand, only in combination were nec-1 and qVD able to reduce the cell death induced by pep5-cpp in HeLa cells. Nec-1, qVD, or SB203580 treatment alone was not effective in blocking pep5-cpp-induced cell death (Fig. 14).

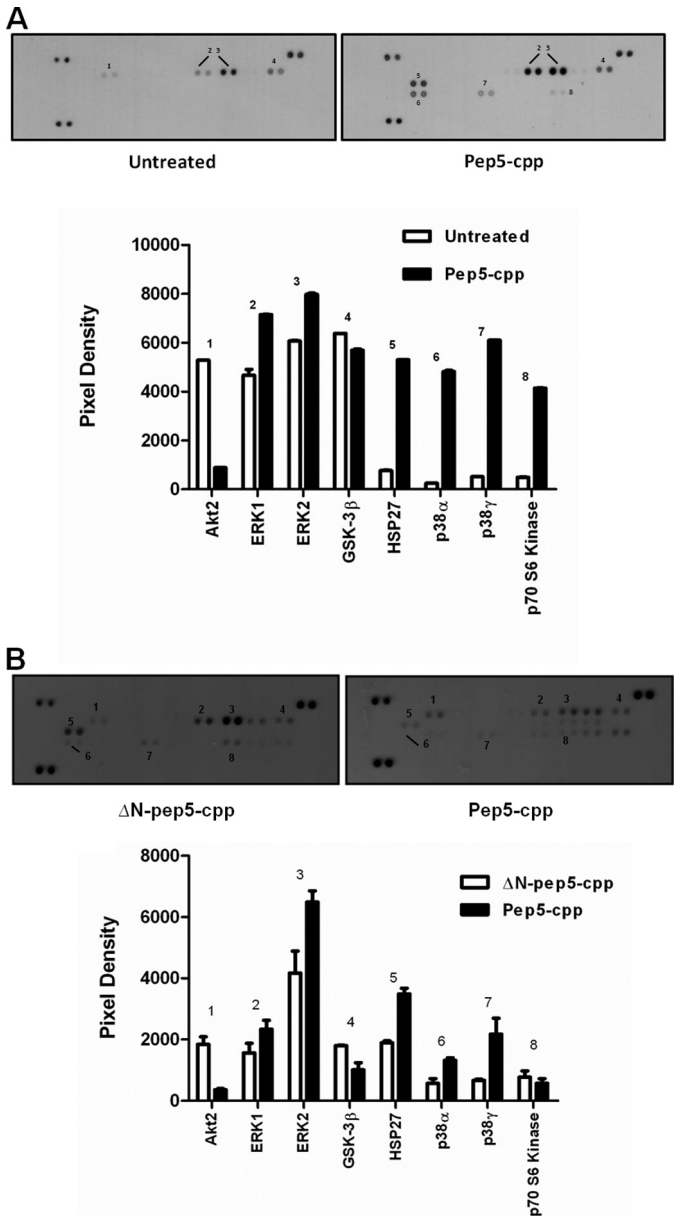

FIGURE 12. **Effect of pep5-cpp in the phosphorylation of specific human MAPKs or their substrates.** HeLa cells were treated or not with peptide 5 (*A*) and ΔN-pep5-cpp (*B*) for 10 min (100 μM). All arrays were incubated with 200 μg of lysate. Δ*N-pep5*, pep5-cpp without one amino acid in the N terminus. The assayed MAPKs and targets included Akt1, Akt2, Akt3, Akt pan, CREB, ERK1, ERK2, GSK-3α/β, GSK-3β, HSP27, JNK1, JNK2, JNK3, JNK pan, MKK3, MKK6, MSK2, p38α, p38β, p38δ, p38γ, p53, p70 S6K, RSK1, RSK2, and TOR. *Error bars*, S.E.

DISCUSSION

In the present study, several novel intracellular peptides were identified in HeLa cells. The relative levels of some of these intracellular peptides appear to fluctuate throughout the cell cycle, which resembles that which is already well established for proteins controlling cell cycle progression. Whereas the broad biological significance of these findings remains elusive, to our knowledge this is the first report to describe fluctuation in the relative levels of intracellular peptides during the cell cycle progression of HeLa cells.

The relative level of the peptide WELVVLGKL (pep5) increases 2-fold in the S phase of HeLa cell cycle, compared with asynchronous cells. Reintroduction of pep5 in HeLa or several additional tumor cell lines induces cell death, suggesting its functionality. In a previous study in HEK293T cells, the concentration of the intracellular peptide VFD-7 was determined to be ~16 μM (27). It is possible that the minimal effective pharmacological dose of pep5 that induces cell death in MDA-MB-231 cells (~25 μM) could be occurring within cells. Differences in the kinetics of administration and/or coupling to a transport mechanism could be related to the distinctive efficacy of pep5 seen in the tumor cell lines investigated in this study. A high structural specificity was observed for pep5, based on the finding that a single amino acid removal, modification, or substitution in the minimal active sequence (WELVVL) reduced or abolished pep5 cell death activity. Therefore, it is also possible that differences in the efficacy of pep5 observed between cell lines are due to variation in the activity of proteases and/or peptidases. Indeed, it has been shown previously that oligopeptidases (24, 25) as well as the proteasome (15, 48) can metabolize a number of intracellular peptides.

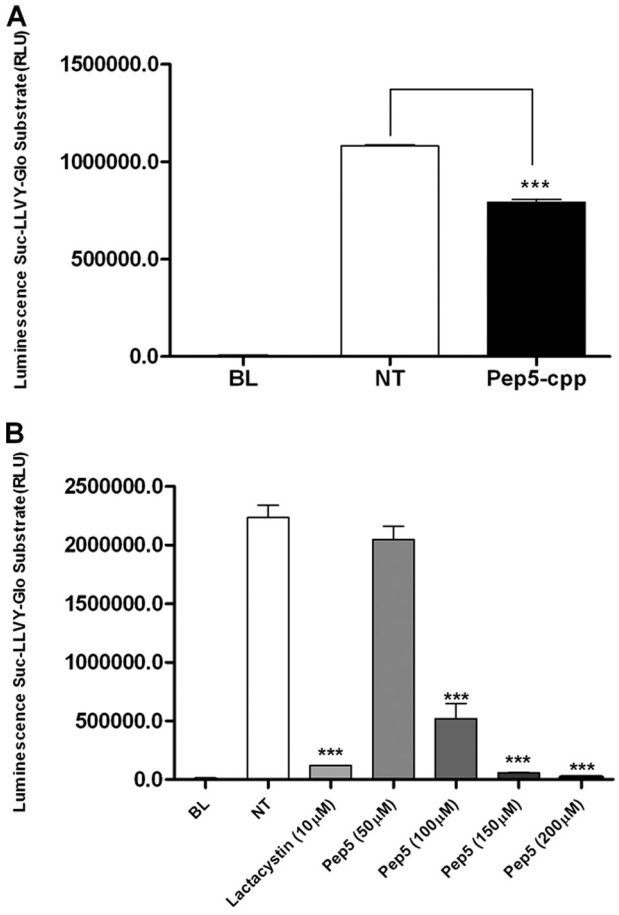

FIGURE 13. **Proteolytic activities of the proteasome in HeLa cells treated or not with pep5-cpp.** Proteasome chymotrypsin activity was measured in aliquots of cell lysates containing 20 μg of protein as described under "Experimental Procedures." *A*, whole HeLa cells were treated with pep5-cpp (100 μM) for 24 h, and the proteasome activity was measured in the cell extracts. *B*, the proteasome activity was measured in the HeLa cell extracts in the presence or absence of pep5 at the indicated concentrations. Lactacystin (10 μM) was used as a positive control. *NT*, not treated; *BL*, blank. *RLU*, relative light units. *Error bars*, S.E.

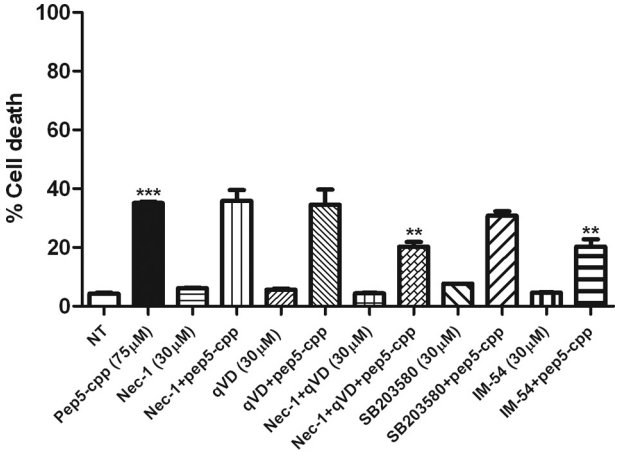

FIGURE 14. **Effect of specific inhibitors of cell death on pep5-cpp activity.** HeLa cells were pretreated with nec-1, qVD, SB203580, or IM-54 (30 μM, 1 h), and then pep5-cpp (75 μM) was added to the medium containing one or more inhibitors. After treatment with pep5-cpp (~4 h), the cells were analyzed by flow cytometry. The data shown here are representative of three experiments performed in triplicate, and the results were considered significant when p was <0.01 (**) or <0.001 (***). *Error bars*, S.E.

Pharmacological examination conducted in HeLa cells suggests that IM-54, a potent and selective inhibitor of oxidative stress-induced necrosis (47), efficiently blocked the cell death activity of pep5. IM-54 selectively inhibits oxidative stress-induced necrosis, as observed in ischemia-reperfusion injury caused by heart attack, and does not inhibit caspase-dependent apoptosis (47). IM-54 is suggested to directly interact with mitochondrial protein(s), which may therefore play a critical role in induction of necrosis. Some studies have demonstrated that necrosis induced by H_2O_2 treatment in HL60 cells also is inhibited by IM-54 (47, 49). Together, these data suggest that pep5 can trigger cell death through the oxidative stress pathway.

Other pathways may also be involved in the induction of cell death by pep5. The simultaneous inhibition of necroptosis and caspase activity by a combination of nec-1 and qVD inhibitors efficiently blocked pep5-cpp cell death activity. Neither of these inhibitors individually reduced cell death induced by pep5-cpp. Mixed type cell death modes containing features of both forms of cell death have been reported and named "aponecrosis." This form of cell death may represent aborted or partially executed apoptotic programs, which occur in the context of a final necrotic outcome (50, 51). The existence of necrotic cell death pathways regulated by an intrinsic death program distinct from that of apoptosis has also been proposed and named necroptosis (52). In apoptosis, caspases 3/7 are effector caspases involved in both the intrinsic and extrinsic pathways. Caspase 8 is involved in the extrinsic apoptotic pathway, and it is activated by ligand binding to membrane-associated death receptors, whereas caspase 9 participates in the intrinsic apoptotic pathway, and it is activated by mitochondrial perturbation, which causes cytochrome *c* release (53–56).

The phosphorylation levels of only six MAPKs or their substrates were affected by pep5 among the 26 proteins evaluated, including Akt2 inhibition and p38γ and p38α activation. It is known that Akt2-deficient mice have an increase in apoptotic cell death in the aorta, whereas the knockdown of all three isoforms of Akt (Akt1/Akt2/Akt3) induces apoptosis in several human tumor cell lines (57). On the other hand, Akt2 overexpression causes an increase in adhesion, invasion, and metastasis in ovarian and human breast cancer cells (58, 59). Other reports show that Akt2 knockdown in non-small cell lung cancer simultaneously causes cleavage of one antiapoptotic protein, cytochrome *c* release, and caspase activation (60). In asynchronous HeLa cells, pep5 was not able to induce cytochrome *c* release (data not shown). pep5 has a similar effect in HeLa cells, inhibiting Akt2 and activating caspase 9. Moreover, mitogen-activated protein kinases such as p38γ and p38α were activated by treatment of HeLa cells with pep5, suggesting that pep5 induces a cross-talk in proapoptotic pathways. Some studies suggest that p38γ is regulated by hypoxia, decreasing the levels of cyclin D1 in PC12 cells, and by ionizing radiation in NIH-3T3 cells, inducing cell cycle arrest (61, 62). Furthermore, when p38α is inhibited, it blocks a checkpoint in G_2/M after ultraviolet radiation in murine and human cells (63). Here, when HeLa cells were treated with the specific p38 inhibitor SB203580, no inhibition of pep5-cpp cell death activity was observed. Therefore, the present results do not suggest that Akt2 inhibition or

```
119 LTAEKLCIYTDNSIRPEELLQMELLLVNKLKWNLAAMTPHDFIEHFLSKMPEAEENKQII 178 CCND1_HUMAN
118 LTAEKLCIYTDNSIKPQELLEWELVVLGKLKWNLAAVTPHDFIEHILRKLPQQREKLSLI 177 CCND2_HUMAN
119 LTIEKLCIYTDHAVSPRQLRDWEVLVLGKLKWDLAAVIAHDFLAFILHRLSLPRDRQALV 178 CCND3_HUMAN
    ** ********.:: *.:* : *:::: ****:***:  ***: .:* ::   .:.  ::
```

FIGURE 15. **Sequence alignment for cyclins D.** Sequences (in FASTA format) or UniProt identifiers of the three human cyclins D (CCND1, CCND2, and CCND3). Note the similarity in amino acids among the D1, D2, and D3 in humans (*). The sequence *underlined* in *green* corresponds to pep5 identity, which is only present in cyclin D2.

p38γ/p38α activation are key effectors of pep5-cpp cell death activity in HeLa cells. One exciting possibility is that endogenous pep5 alters cell-specific signaling pathways without causing cell death.

pep5-cpp induced cell death in both C6 rat glioma cells and in the rat glioblastoma *in vivo*. Glioblastoma is the most malignant astrocytoma in humans. Several drugs have been developed to treat gliomas, such as inhibitors of key oncogenic signaling pathways, apoptosis-inducing drugs, and DNA-damaging drugs (64–67). The group of animals treated with pep5-cpp showed a decrease of ~50% of the tumor volume when compared with the control group. It was interesting to note that pep5-cpp induced an increase in macrophage-like cells in the tumor area, probably due to induction of cell death. These data suggest that pep5-cpp also could be a new pharmacological tool in glioblastoma treatment.

pep5 was shown to inhibit the chymotrypsin activity of the proteasome, suggesting the possibility of an inhibitory feedback mechanism over the proteasome during cyclin D2 degradation. Cell cycle, gene expression, and apoptosis are events regulated by the cleavage of several proteins by the ubiquitin-proteasome system, including transcription factors, cyclins, and cyclin-dependent kinase inhibitors (68, 69). Several transcription factors, such as NF-κB, are involved in the control of the immune response, cell proliferation, and programmed cell death. In the development of malignancy, these proteins can alter the regulation of other factors, contributing to tumorigenesis (70–72). Cyclins are degraded by the proteasome in order to permit the exit of cells from mitosis and their entry into another round of the cell cycle (73). Five main classes of mammalian cyclins have been described. Cyclins C, D (1, 2, and 3), and E act during the G_1 phase and regulate the transition from G_1 to S phase. In contrast, cyclins A and B (1 and 2) have activity during the S and G_2 phases and are regulators of entry into mitosis (74–76). The expression levels of cyclin-dependent kinase inhibitors, including p21, p27, and p57, also are degraded by the ubiquitin-proteasome system, and this control is an important event for cell regulation (77). In tumor cells, there is uncontrolled cell growth and nearly constant proliferation and division, which requires extensive protein degradation. For this reason, proteasome inhibitors have been used as anti-tumor agents, helping to regulate the uncontrolled cell growth and inducing apoptosis in several tumor cells (78–81).

The sequence of pep5 is present only in cyclin D2 and is not found in the other cyclins (Fig. 15). There is total homology of the pep5 sequence within cyclin D2 from a wide range of organisms, including humans, rats, bovines, mice, and chickens, suggesting its biological significance. Cyclin D2 must be degraded by the proteasome during G_1/S transition to allow cell cycle progression (82), which suggests that pep5 can be endogenously generated by the proteasome. The proteasome has been shown to regulate the levels of most intracellular peptides (14, 15), and pep5 was seen by bioinformatics analysis to be compatible with generation by the proteasome, followed by aminopeptidase activity (data not shown). Therefore, it is possible that proteasome inhibitors could alter levels of pep5, which could contribute to cell death.

In the maintenance of mitochondrial protein stability, proteases degrade proteins into peptides that are exported from the mitochondrial matrix into the intermembrane space by ABC transporters and reach the cytosol by passive diffusion. Haynes *et al.* (83) demonstrated by genetic analysis of *Caenorhabditis elegans* that under stress of mitochondrial protein misfolding, signal peptides generated by the mitochondrial ATP-dependent proteolytic complex can activate the cell genome, providing a mechanism of intracellular communication among mitochondria, cytosol, and nucleus. As a consequence, the organelle can react against the loss of thermodynamic stability and the propensity of proteins to aggregate, inducing the expression of a nuclear encoded protein gene termed ubiquitin-like ClpXP, which is activated by a homeobox containing the transcription factor bZIP. bZIP is believed to be activated by a pathway that involves different peptides produced by ATP-dependent Clp proteases. The combined expression of these proteins using intracellular signal peptides represents the cell response toward the damage produced by irreversible aggregates and protein misfolding affecting cell functions and survival (83). These findings corroborate previous evidence that endogenous intracellular peptides are probably functional and of biological significance (84).

In summary, these findings suggest that pep5 is a novel bioactive intracellular peptide. There is an exciting possibility that pep5 could serve as a novel prototype molecule in pharmacology and therapeutics.

Acknowledgments—We thank Andrea S. Heimann (Proteimax Biotechnology LTDA) for scientific advice and peptide design and supply. We also thank Professor Edna T. Kimura for generously providing NThy-ori 3-1, KTC-2, and TPC-1 cell lines and for assistance with flow cytometry; Adilson Kleber Ferreira, Ph.D., for providing additional tumor cell lines; Marcella Faria, Ph.D., and Professor Hugo A. Armelin for critical discussions and suggestions and for providing the p38 inhibitor; and Joao Gustavo Pessini Amarante Mendes for providing the qVD inhibitor. We also thank Professor Lloyd D. Fricker for outstanding and helpful discussions during manuscript preparation.

REFERENCES

1. Paz, P., Brouwenstijn, N., Perry, R., and Shastri, N. (1999) Discrete proteolytic intermediates in the MHC class I antigen processing pathway and MHC I-dependent peptide trimming in the ER. *Immunity* **11,** 241–251
2. Rock, K. L., and Goldberg, A. L. (1999) Degradation of cell proteins and the generation of MHC class I-presented peptides. *Annu. Rev. Immunol.* **17,**

739–779
3. Hershko, A. (2005) The ubiquitin system for protein degradation and some of its roles in the control of the cell division cycle. *Cell Death Differ.* **12,** 1191–1197
4. Goldberg, A. L. (2012) Development of proteasome inhibitors as research tools and cancer drugs. *J. Cell Biol.* **199,** 583–588
5. Kisselev, A. F., Akopian, T. N., and Goldberg, A. L. (1998) Range of sizes of peptide products generated during degradation of different proteins by archaeal proteasomes. *J. Biol. Chem.* **273,** 1982–1989
6. Kisselev, A. F., Akopian, T. N., Woo, K. M., and Goldberg, A. L. (1999) The sizes of peptides generated from protein by mammalian 26 and 20 S proteasomes. Implications for understanding the degradative mechanism and antigen presentation. *J. Biol. Chem.* **274,** 3363–3371
7. Rammensee, H. G. (2002) Survival of the fitters. *Nature* **419,** 443–445
8. Geier, E., Pfeifer, G., Wilm, M., Lucchiari-Hartz, M., Baumeister, W., Eichmann, K., and Niedermann, G. (1999) A giant protease with potential to substitute for some functions of the proteasome. *Science* **283,** 978–981
9. Suraweera, A., Münch, C., Hanssum, A., and Bertolotti, A. (2012) Failure of amino acid homeostasis causes cell death following proteasome inhibition. *Mol. Cell* **48,** 242–253
10. Reits, E., Neijssen, J., Herberts, C., Benckhuijsen, W., Janssen, L., Drijfhout, J. W., and Neefjes, J. (2004) A major role for TPPII in trimming proteasomal degradation products for MHC class I antigen presentation. *Immunity* **20,** 495–506
11. Reits, E., Griekspoor, A., Neijssen, J., Groothuis, T., Jalink, K., van Veelen, P., Janssen, H., Calafat, J., Drijfhout, J. W., and Neefjes, J. (2003) Peptide diffusion, protection, and degradation in nuclear and cytoplasmic compartments before antigen presentation by MHC class I. *Immunity* **18,** 97–108
12. Beninga, J., Rock, K. L., and Goldberg, A. L. (1998) Interferon-γ can stimulate post-proteasomal trimming of the N terminus of an antigenic peptide by inducing leucine aminopeptidase. *J. Biol. Chem.* **273,** 18734–18742
13. Kravtsova-Ivantsiv, Y., Cohen, S., and Ciechanover, A. (2009) Modification by single ubiquitin moieties rather than polyubiquitination is sufficient for proteasomal processing of the p105 NF-κB precursor. *Mol. Cell* **33,** 496–504
14. Gelman, J. S., Dasgupta, S., Berezniuk, I., and Fricker, L. D. (2013) Analysis of peptides secreted from cultured mouse brain tissue. *Biochim. Biophys. Acta* **1834,** 2408–2417
15. Fricker, L. D., Gelman, J. S., Castro, L. M., Gozzo, F. C., and Ferro, E. S. (2012) Peptidomic analysis of HEK293T cells: effect of the proteasome inhibitor epoxomicin on intracellular peptides. *J. Proteome Res.* **11,** 1981–1990
16. Ferro, E. S., Hyslop, S., and Camargo, A. C. (2004) Intracellullar peptides as putative natural regulators of protein interactions. *J. Neurochem.* **91,** 769–777
17. Burns-Hamuro, L. L., Ma, Y., Kammerer, S., Reineke, U., Self, C., Cook, C., Olson, G. L., Cantor, C. R., Braun, A., and Taylor, S. S. (2003) Designing isoform-specific peptide disruptors of protein kinase A localization. *Proc. Natl. Acad. Sci. U.S.A.* **100,** 4072–4077
18. Churchill, E. N., Qvit, N., and Mochly-Rosen, D. (2009) Rationally designed peptide regulators of protein kinase C. *Trends Endocrinol. Metab.* **20,** 25–33
19. Rioli, V., Gozzo, F. C., Heimann, A. S., Linardi, A., Krieger, J. E., Shida, C. S., Almeida, P. C., Hyslop, S., Eberlin, M. N., and Ferro, E. S. (2003) Novel natural peptide substrates for endopeptidase 24.15, neurolysin, and angiotensin-converting enzyme. *J. Biol. Chem.* **278,** 8547–8555
20. Heimann, A. S., Gomes, I., Dale, C. S., Pagano, R. L., Gupta, A., de Souza, L. L., Luchessi, A. D., Castro, L. M., Giorgi, R., Rioli, V., Ferro, E. S., and Devi, L. A. (2007) Hemopressin is an inverse agonist of CB1 cannabinoid receptors. *Proc. Natl. Acad. Sci. U.S.A.* **104,** 20588–20593
21. Dodd, G. T., Mancini, G., Lutz, B., and Luckman, S. M. (2010) The peptide hemopressin acts through CB1 cannabinoid receptors to reduce food intake in rats and mice. *J. Neurosci.* **30,** 7369–7376
22. Gomes, I., Grushko, J. S., Golebiewska, U., Hoogendoorn, S., Gupta, A., Heimann, A. S., Ferro, E. S., Scarlata, S., Fricker, L. D., and Devi, L. A. (2009) Novel endogenous peptide agonists of cannabinoid receptors. *FASEB J.* **23,** 3020–3029
23. Cunha, F. M., Berti, D. A., Ferreira, Z. S., Klitzke, C. F., Markus, R. P., and Ferro, E. S. (2008) Intracellular peptides as natural regulators of cell signaling. *J. Biol. Chem.* **283,** 24448–24459
24. Berti, D. A., Morano, C., Russo, L. C., Castro, L. M., Cunha, F. M., Zhang, X., Sironi, J., Klitzke, C. F., Ferro, E. S., and Fricker, L. D. (2009) Analysis of intracellular substrates and products of thimet oligopeptidase in human embryonic kidney 293 cells. *J. Biol. Chem.* **284,** 14105–14116
25. Russo, L. C., Castro, L. M., Gozzo, F. C., and Ferro, E. S. (2012) Inhibition of thimet oligopeptidase by siRNA alters specific intracellular peptides and potentiates isoproterenol signal transduction. *FEBS Lett.* **586,** 3287–3292
26. Berti, D. A., Russo, L. C., Castro, L. M., Cruz, L., Gozzo, F. C., Heimann, J. C., Lima, F. B., Oliveira, A. C., Andreotti, S., Prada, P. O., Heimann, A. S., and Ferro, E. S. (2012) Identification of intracellular peptides in rat adipose tissue: insights into insulin resistance. *Proteomics* **12,** 2668–2681
27. Russo, L. C., Asega, A. F., Castro, L. M., Negraes, P. D., Cruz, L., Gozzo, F. C., Ulrich, H., Camargo, A. C., Rioli, V., and Ferro, E. S. (2012) Natural intracellular peptides can modulate the interactions of mouse brain proteins and thimet oligopeptidase with 14-3-3ϵ and calmodulin. *Proteomics* **12,** 2641–2655
28. Che, F. Y., Biswas, R., and Fricker, L. D. (2005) Relative quantitation of peptides in wild-type and Cpe(fat/fat) mouse pituitary using stable isotopic tags and mass spectrometry. *J. Mass Spectrom.* **40,** 227–237
29. Morano, C., Zhang, X., and Fricker, L. D. (2008) Multiple isotopic labels for quantitative mass spectrometry. *Anal. Chem.* **80,** 9298–9309
30. Zhang, R., Sioma, C. S., Thompson, R. A., Xiong, L., and Regnier, F. E. (2002) Controlling deuterium isotope effects in comparative proteomics. *Anal. Chem.* **74,** 3662–3669
31. Gallo, C. J., Koza, R. A., and Herbst, E. J. (1986) Polyamines and HeLa-cell DNA replication. *Biochem. J.* **238,** 37–42
32. Zhou, J. Y., Ma, W. L., Liang, S., Zeng, Y., Shi, R., Yu, H. L., Xiao, W. W., and Zheng, W. L. (2009) Analysis of microRNA expression profiles during the cell cycle in synchronized HeLa cells. *BMB Rep.* **42,** 593–598
33. Benda, P., Lightbody, J., Sato, G., Levine, L., and Sweet, W. (1968) Differentiated rat glial cell strain in tissue culture. *Science* **161,** 370–371
34. Udenfriend, S., Stein, S., Böhlen, P., Dairman, W., Leimgruber, W., and Weigele, M. (1972) Fluorescamine: a reagent for assay of amino acids, peptides, proteins, and primary amines in the picomole range. *Science* **178,** 871–872
35. Castro, L. M., Berti, D. A., Russo, L. C., Coelho, V., Gozzo, F. C., Oliveira, V., and Ferro, E. S. (2010) Similar intracellular peptide profile of TAP1/β2 microglobulin double-knockout mice and C57BL/6 wild-type mice as revealed by peptidomic analysis. *AAPS J.* **12,** 608–616
36. Che, F. Y., Zhang, X., Berezniuk, I., Callaway, M., Lim, J., and Fricker, L. D. (2007) Optimization of neuropeptide extraction from the mouse hypothalamus. *J. Proteome Res.* **6,** 4667–4676
37. Wardman, J., and Fricker, L. D. (2011) Quantitative peptidomics of mice lacking peptide-processing enzymes. *Methods Mol. Biol.* **768,** 307–323
38. Wang, G., Sun, W., Luo, Y., and Fang, N. (2010) Resolving rotational motions of nano-objects in engineered environments and live cells with gold nanorods and differential interference contrast microscopy. *J. Am. Chem. Soc.* **132,** 16417–16422
39. Ziegler, A., Nervi, P., Dürrenberger, M., and Seelig, J. (2005) The cationic cell-penetrating peptide CPP(TAT) derived from the HIV-1 protein TAT is rapidly transported into living fibroblasts: optical, biophysical, and metabolic evidence. *Biochemistry* **44,** 138–148
40. Wender, P. A., Mitchell, D. J., Pattabiraman, K., Pelkey, E. T., Steinman, L., and Rothbard, J. B. (2000) The design, synthesis, and evaluation of molecules that enable or enhance cellular uptake: peptoid molecular transporters. *Proc. Natl. Acad. Sci. U.S.A.* **97,** 13003–13008
41. Bradford, M. M. (1976) A rapid and sensitive method for the quantitation of microgram quantities of protein utilizing the principle of protein-dye binding. *Anal. Biochem.* **72,** 248–254
42. Zarubin, T., and Han, J. (2005) Activation and signaling of the p38 MAP kinase pathway. *Cell Res.* **15,** 11–18
43. Degterev, A., Huang, Z., Boyce, M., Li, Y., Jagtap, P., Mizushima, N., Cuny, G. D., Mitchison, T. J., Moskowitz, M. A., and Yuan, J. (2005) Chemical inhibitor of nonapoptotic cell death with therapeutic potential for ische-

mic brain injury. *Nat. Chem. Biol.* **1,** 112–119
44. Caserta, T. M., Smith, A. N., Gultice, A. D., Reedy, M. A., and Brown, T. L. (2003) Q-VD-OPh, a broad spectrum caspase inhibitor with potent anti-apoptotic properties. *Apoptosis* **8,** 345–352
45. Cuenda, A., Rouse, J., Doza, Y. N., Meier, R., Cohen, P., Gallagher, T. F., Young, P. R., and Lee, J. C. (1995) SB 203580 is a specific inhibitor of a MAP kinase homologue which is stimulated by cellular stresses and interleukin-1. *FEBS Lett.* **364,** 229–233
46. Lali, F. V., Hunt, A. E., Turner, S. J., and Foxwell, B. M. (2000) The pyridinyl imidazole inhibitor SB203580 blocks phosphoinositide-dependent protein kinase activity, protein kinase B phosphorylation, and retinoblastoma hyperphosphorylation in interleukin-2-stimulated T cells independently of p38 mitogen-activated protein kinase. *J. Biol. Chem.* **275,** 7395–7402
47. Sodeoka, M., and Dodo, K. (2010) Development of selective inhibitors of necrosis. *Chem. Rec.* **10,** 308–314
48. Gelman, J. S., Sironi, J., Berezniuk, I., Dasgupta, S., Castro, L. M., Gozzo, F. C., Ferro, E. S., and Fricker, L. D. (2013) Alterations of the intracellular peptidome in response to the proteasome inhibitor bortezomib. *PLoS One* **8,** e53263
49. Dodo, K., Katoh, M., Shimizu, T., Takahashi, M., and Sodeoka, M. (2005) Inhibition of hydrogen peroxide-induced necrotic cell death with 3-amino-2-indolylmaleimide derivatives. *Bioorg. Med. Chem. Lett.* **15,** 3114–3118
50. Wang, X., Ryter, S. W., Dai, C., Tang, Z. L., Watkins, S. C., Yin, X. M., Song, R., and Choi, A. M. (2003) Necrotic cell death in response to oxidant stress involves the activation of the apoptogenic caspase-8/bid pathway. *J. Biol. Chem.* **278,** 29184–29191
51. Ryter, S. W., Kim, H. P., Hoetzel, A., Park, J. W., Nakahira, K., Wang, X., and Choi, A. M. (2007) Mechanisms of cell death in oxidative stress. *Antioxid. Redox Signal.* **9,** 49–89
52. Kitanaka, C., and Kuchino, Y. (1999) Caspase-independent programmed cell death with necrotic morphology. *Cell Death Differ.* **6,** 508–515
53. Hengartner, M. O. (2000) The biochemistry of apoptosis. *Nature* **407,** 770–776
54. Jin, Z., and El-Deiry, W. S. (2005) Overview of cell death signaling pathways. *Cancer Biol. Ther.* **4,** 139–163
55. Peter, M. E., and Krammer, P. H. (2003) The CD95(APO-1/Fas) DISC and beyond. *Cell Death Differ.* **10,** 26–35
56. Li, P., Nijhawan, D., Budihardjo, I., Srinivasula, S. M., Ahmad, M., Alnemri, E. S., and Wang, X. (1997) Cytochrome *c* and dATP-dependent formation of Apaf-1/caspase-9 complex initiates an apoptotic protease cascade. *Cell* **91,** 479–489
57. Koseoglu, S., Lu, Z., Kumar, C., Kirschmeier, P., and Zou, J. (2007) AKT1, AKT2 and AKT3-dependent cell survival is cell line-specific and knockdown of all three isoforms selectively induces apoptosis in 20 human tumor cell lines. *Cancer Biol. Ther.* **6,** 755–762
58. Shen, Y. H., Zhang, L., Ren, P., Nguyen, M. T., Zou, S., Wu, D., Wang, X. L., Coselli, J. S., and LeMaire, S. A. (2013) AKT2 confers protection against aortic aneurysms and dissections. *Circ. Res.* **112,** 618–632
59. Arboleda, M. J., Lyons, J. F., Kabbinavar, F. F., Bray, M. R., Snow, B. E., Ayala, R., Danino, M., Karlan, B. Y., and Slamon, D. J. (2003) Overexpression of AKT2/protein kinase Bbeta leads to up-regulation of β1 integrins, increased invasion, and metastasis of human breast and ovarian cancer cells. *Cancer Res.* **63,** 196–206
60. Lee, M. W., Kim, D. S., Lee, J. H., Lee, B. S., Lee, S. H., Jung, H. L., Sung, K. W., Kim, H. T., Yoo, K. H., and Koo, H. H. (2011) Roles of AKT1 and AKT2 in non-small cell lung cancer cell survival, growth, and migration. *Cancer Sci.* **102,** 1822–1828
61. Conrad, P. W., Freeman, T. L., Beitner-Johnson, D., and Millhorn, D. E. (1999) EPAS1 trans-activation during hypoxia requires p42/p44 MAPK. *J. Biol. Chem.* **274,** 33709–33713
62. Wang, X., McGowan, C. H., Zhao, M., He, L., Downey, J. S., Fearns, C., Wang, Y., Huang, S., and Han, J. (2000) Involvement of the MKK6-p38γ cascade in γ-radiation-induced cell cycle arrest. *Mol. Cell Biol.* **20,** 4543–4552
63. Bulavin, D. V., Higashimoto, Y., Popoff, I. J., Gaarde, W. A., Basrur, V., Potapova, O., Appella, E., and Fornace, A. J., Jr. (2001) Initiation of a G_2/M checkpoint after ultraviolet radiation requires p38 kinase. *Nature* **411,** 102–107
64. Ferguson, S., and Lesniak, M. S. (2007) Convection enhanced drug delivery of novel therapeutic agents to malignant brain tumors. *Curr. Drug Deliv.* **4,** 169–180
65. Wen, P. Y., Kesari, S., and Drappatz, J. (2006) Malignant gliomas: strategies to increase the effectiveness of targeted molecular treatment. *Expert Rev. Anticancer Ther.* **6,** 733–754
66. Jiang, H., Alonso, M. M., Gomez-Manzano, C., Piao, Y., and Fueyo, J. (2006) Oncolytic viruses and DNA-repair machinery: overcoming chemoresistance of gliomas. *Expert Rev. Anticancer Ther.* **6,** 1585–1592
67. Kim, L., and Glantz, M. (2006) Chemotherapeutic options for primary brain tumors. *Curr. Treat. Options Oncol.* **7,** 467–478
68. Hershko, A. (1997) Roles of ubiquitin-mediated proteolysis in cell cycle control. *Curr. Opin. Cell Biol.* **9,** 788–799
69. Chun, K. T., Mathias, N., and Goebl, M. G. (1996) Ubiquitin-dependent proteolysis and cell cycle control in yeast. *Prog. Cell Cycle Res.* **2,** 115–127
70. Murray, R. Z., and Norbury, C. (2000) Proteasome inhibitors as anti-cancer agents. *Anticancer Drugs* **11,** 407–417
71. Spataro, V., Norbury, C., and Harris, A. L. (1998) The ubiquitin-proteasome pathway in cancer. *Br. J. Cancer* **77,** 448–455
72. Karin, M., Cao, Y., Greten, F. R., and Li, Z. W. (2002) NF-kappaB in cancer: from innocent bystander to major culprit. *Nat. Rev. Cancer* **2,** 301–310
73. Glotzer, M., Murray, A. W., and Kirschner, M. W. (1991) Cyclin is degraded by the ubiquitin pathway. *Nature* **349,** 132–138
74. Sherr, C. J. (1994) G_1 phase progression: cycling on cue. *Cell* **79,** 551–555
75. King, R. W., Jackson, P. K., and Kirschner, M. W. (1994) Mitosis in transition. *Cell* **79,** 563–571
76. Nurse, P. (1994) Ordering S phase and M phase in the cell cycle. *Cell* **79,** 547–550
77. Nakayama, K. (1998) Cip/Kip cyclin-dependent kinase inhibitors: brakes of the cell cycle engine during development. *BioEssays* **20,** 1020–1029
78. Imajoh-Ohmi, S., Kawaguchi, T., Sugiyama, S., Tanaka, K., Omura, S., and Kikuchi, H. (1995) Lactacystin, a specific inhibitor of the proteasome, induces apoptosis in human monoblast U937 cells. *Biochem. Biophys. Res. Commun.* **217,** 1070–1077
79. Adams, J., Palombella, V. J., Sausville, E. A., Johnson, J., Destree, A., Lazarus, D. D., Maas, J., Pien, C. S., Prakash, S., and Elliott, P. J. (1999) Proteasome inhibitors: a novel class of potent and effective antitumor agents. *Cancer Res.* **59,** 2615–2622
80. Drexler, H. C. (1997) Activation of the cell death program by inhibition of proteasome function. *Proc. Natl. Acad. Sci. U.S.A.* **94,** 855–860
81. Sunwoo, J. B., Chen, Z., Dong, G., Yeh, N., Crowl Bancroft, C., Sausville, E., Adams, J., Elliott, P., and Van Waes, C. (2001) Novel proteasome inhibitor PS-341 inhibits activation of nuclear factor-κB, cell survival, tumor growth, and angiogenesis in squamous cell carcinoma. *Clin. Cancer Res.* **7,** 1419–1428
82. Chen, B. B., Glasser, J. R., Coon, T. A., Zou, C., Miller, H. L., Fenton, M., McDyer, J. F., Boyiadzis, M., and Mallampalli, R. K. (2012) F-box protein FBXL2 targets cyclin D2 for ubiquitination and degradation to inhibit leukemic cell proliferation. *Blood* **119,** 3132–3141
83. Haynes, C. M., Yang, Y., Blais, S. P., Neubert, T. A., and Ron, D. (2010) The matrix peptide exporter HAF-1 signals a mitochondrial UPR by activating the transcription factor ZC376.7 in *C. elegans*. *Mol. Cell* **37,** 529–540
84. Ferro, E. S., Rioli, V., Castro, L. M., and Fricker, L. D. (2014) Intracellular peptides: from discovery to function. *EuPA Open Proteomics* **3,** 143–151